Greenhouse gas emissions and organic carbon content in freshwater ponds, lakes, and rivers in the Northeastern Siberian tundra

By
Henk Lenderink
3699897

Utrecht University, MSc Thesis
Earth, Life and Climate

April 2017

Supervised by:
Prof. dr. J.B.M. Middelburg
Dr. J.E. Vonk
Dr. J.F. Dean

Abstract

Although permafrost soils are one of the most important carbon reservoir system on earth, permafrost carbon is rarely integrated in analyses of future atmospheric carbon concentrations due to the complexity of different water bodies. Water bodies cover a major part of Arctic permafrost regions and have an important role in the permafrost carbon cycle. The amount and type of carbon concentrations in permafrost water bodies can have a large impact on the release of future atmospheric greenhouse gases.

In order to contribute to a better understanding in permafrost freshwater carbon concentrations, over 100 water and gas samples were analysed on POC, DOC, CH_4, and CO_2 for lakes, ponds, and streams in the Kytalyk nature reserve (Northeastern Siberian tundra). Carbon content of the different water bodies were compared to each other, and to other measured parameters such as salinity, pH, and surface area. Also stable isotope measurements ($\delta^{18}O$ and $\delta^{2}H$) were analysed in order to obtain a local evaporation line.

Results of this research show not only a higher carbon content, as well as a higher ratio of greenhouse gases (CH_4 and CO_2) in respect to other carbon forms for ponds compared to lakes and streams. The CH_4 concentration in all different water bodies seems equally or even more important as a greenhouse gas compared to CO_2 concentrations. The amount of DOC is higher compared to the POC concentrations for all of the measured water bodies. A clear correlation was found between the surface area and pH of the freshwater system and the total carbon content of the pond systems. Stable isotope measurements suggest that ponds are primarily affected by summer precipitation and evapotranspiration, whereas lakes are mainly influenced by thawed ice from ice wedges in the soil.

Universiteit Utrecht

VU

Table of contents

1. Introduction

One of the most important issues threatening the planet in the present time is anthropogenic climate change. A major component driving climate variability is the atmospheric concentration of carbon, which is highly correlated to the global carbon cycle (Mackenzie, 1980). Since the beginning of the Industrial Era (1750 AD), the abundance of well-mixed greenhouse gases such as carbon dioxide (CO_2) and methane (CH_4) have increased substantially (Ciais et al., 2013). For the research of future atmospheric greenhouse gases not only human activities are important, but also the response of the major global carbon reservoir systems (land, ocean, and atmosphere) in respect to climate change (Friedlingstein et al., 2006). The impact of the different reservoir systems is caused by the size, as well as the exchange rate of the system.

Permafrost soils are one of these large carbon reservoir systems, although they are rarely integrated into analyses of future atmospheric carbon concentrations due to their complexity and high uncertainty (Thornton et al., 2016). Permafrost, defined as ground remaining below 0°C for at least two years, occupies almost 25% of the Northern Hemisphere exposed land surface area (Zhang et al., 1999). Of the estimated 1672 Pg (Petagram equals 10^{15} gram) of carbon in the permafrost soils, 818 Pg of carbon is located in the top three meter, which is highly sensitive for microbial activity (Schaefer et al., 2011). This is equivalent to the current amount of carbon in the atmosphere, and is twice as much as all the carbon ever emitted by human activity in modern times (Tarnocai et al., 2009; Schuur and Abbott, 2011). Release of this carbon as CO_2 and CH_4 into the atmosphere can therefore have a large impact on the future carbon cycle and global climate.

Emitted atmospheric CH_4 have a lifetime of about a decade, which is much shorter compared to atmospheric CO_2. Atmospheric CO_2 can stay in the atmosphere for 1000s of years. Still, the greenhouse warming potential on century timescale of CH_4 is about 25 times higher compared to atmospheric CO_2 (EPA, 2017). This is caused by the high energy absorption rate and the close relation of CH_4 with ozone, another greenhouse gas. The global warming potential of N_2O is 265-298 times that of CO_2 (EPA, 2017), although N_2O concentrations in permafrost freshwater bodies are found to be very low (Goovaerts, 2016).

Water bodies cover a major part of permafrost regions and are an important element in the permafrost carbon cycle. The hydrological and carbon cycles in the Arctic are closely linked (Dean et al., 2016). Both surface water and deeper groundwater can potentially transfer respectively younger and older carbon to the aquatic system (Neff et al., 2006). Due to microbial decomposition of the organic carbon, this carbon can be released into the atmosphere.

Most research on permafrost water bodies addresses lakes with a large surface area, as small permafrost ponds (<1000 m^2 surface area and depths measured in decimetres) are invisible for most satellites (Abnizova et al., 2012; Thornton et al., 2016). The underlying processes leading to the release in greenhouse gases are not completely equal for ponds, lakes, and streams (Thornton et al., 2016). Some of these processes, such as seasonal water level, wind speed, and precipitation, have an aberrant effect on the different freshwater bodies due to differences in the conditions of the freshwater bodies. This makes it difficult to estimate the carbon release from permafrost freshwater systems.

To increase the knowledge of carbon concentrations in the permafrost freshwater systems, and fluxes between these systems and the atmosphere, this study will analyse samples from a series of lakes and rivers, as well as samples from small ponds in the Kytalyk nature reserve, located in the Sakha Republic of Russia, a region underlain by continuous permafrost.

During fieldwork in the summer of 2016, over 100 water and gas samples were obtained. Besides these different samples, eddy covariance tower data (CO_2, CH_4, temperature, and wind data) of the same area were collected. The results of the analyses of stable isotope ($\delta^{18}O$ and $\delta^{2}H$), dissolved organic carbon (DOC), particulate organic carbon (POC), and different dissolved gas concentration (CO_2, CH_4 and N_2O) measurements were compared to each other, to other measured parameters in the field, and to data from previous Arctic studies.

The aim of this research is to contribute to a better understanding in the concentration and composition of freshwater carbon at ponds, lakes, and streams in permafrost area. In order to achieve this aim, POC, DOC, CH_4, CO_2, and N_2O concentrations were analysed for the different freshwater bodies. These concentrations were combined for each of the three different water bodies. Differences in both amount and ratio between ponds, lakes, and streams were analysed. Outliers in concentrations were analysed based on measured field parameters. The amount and ratio of carbon concentrations of some of the lake samples were analysed separately due to the occurrence of active thermokarst at these sample locations. Based on the stable isotope measurements, a local evaporation line (LEL) was constructed for northeast Siberia.

2. Background

2.1. Regional Settings

The sample data presented in this study are collected from streams, lakes and ponds in the northeast Siberian tundra (Russia; figure 1), at the Kytalyk Wildlife Reserve (70°83'N, 147°49'E; appendix 1). The sample area is part of the Chokurdakh Scientific Tundra Station, located near the north bank of the Berelekh River in Northeastern Yakutia, Republic of Sakha ("Chokurdakh Scientific Tundra Station," 2014). The Berelekh River is a tributary of the Indigirka River. The research area is located 30 km northwest of Chokurdakh village, 480 km north of the Arctic Circle, and 120 km south of the Arctic Ocean. The fieldwork took place between 31 July and 11 August 2016.

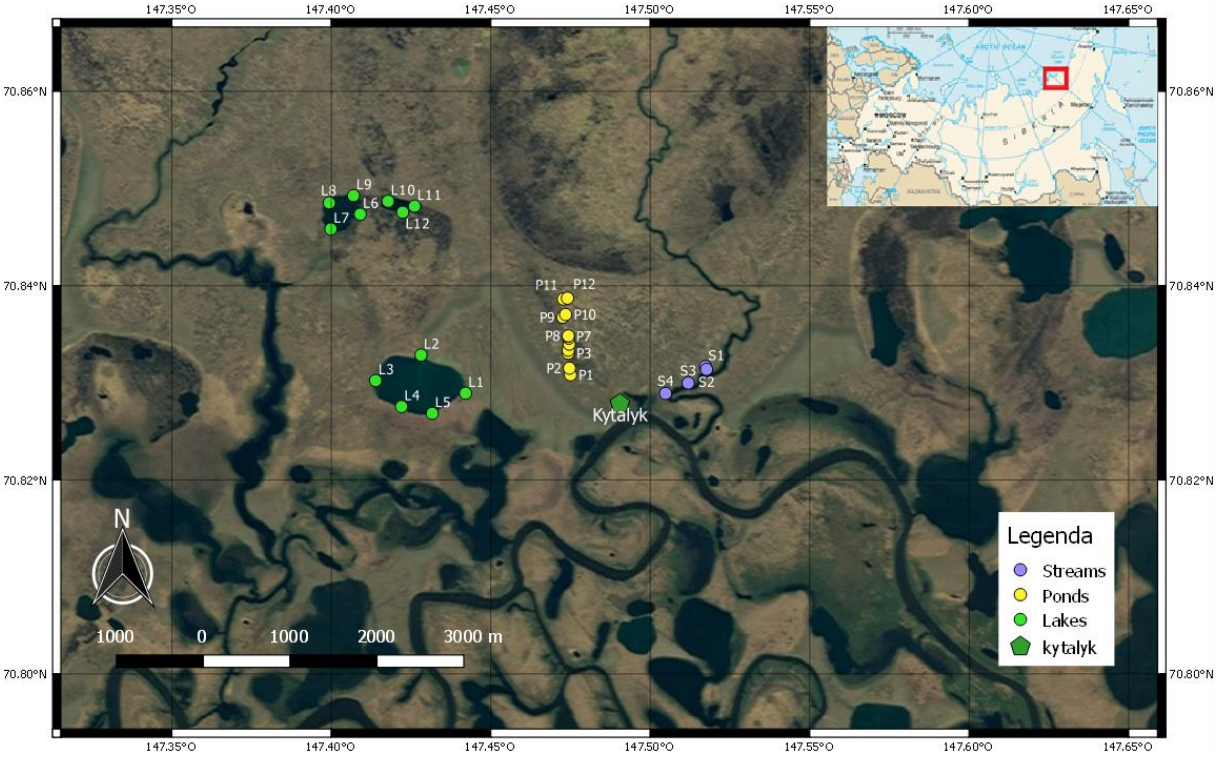

Figure 1. Map of the different sample locations (Northeastern Yakutia, Russia). The green pentagon shape shows the position of the Kytalyk camp (QGIS2.16.3).

According to the World Meteorological Organization, the mean annual air temperature in Chokurdakh is -14.2°C with the highest mean air temperatures in July (+9.7°C), and lowest temperatures in January (-36.6°C). Mean annual precipitation does not exceed 350 mm and most of the precipitation occurs between June and October ("Climate: Chokurdakh", 2016; figure 2). About 50% of the precipitation falls as rain during the summer, the other 50% falls as snow during the rest of the year.

Due to the position of the research area, close to the Arctic Ocean, summer temperatures show a large variability (between 5°C and 25°C; Parmentier et al., 2011). Low temperatures will occur when cold wind is coming from the Arctic Ocean, whereas high temperatures will be the result of wind coming from the warmer Siberian continent. The research area is located in a continuous permafrost zone, with an estimated permafrost thickness of more than 300 meter (Van Huissteden et al., 2005).

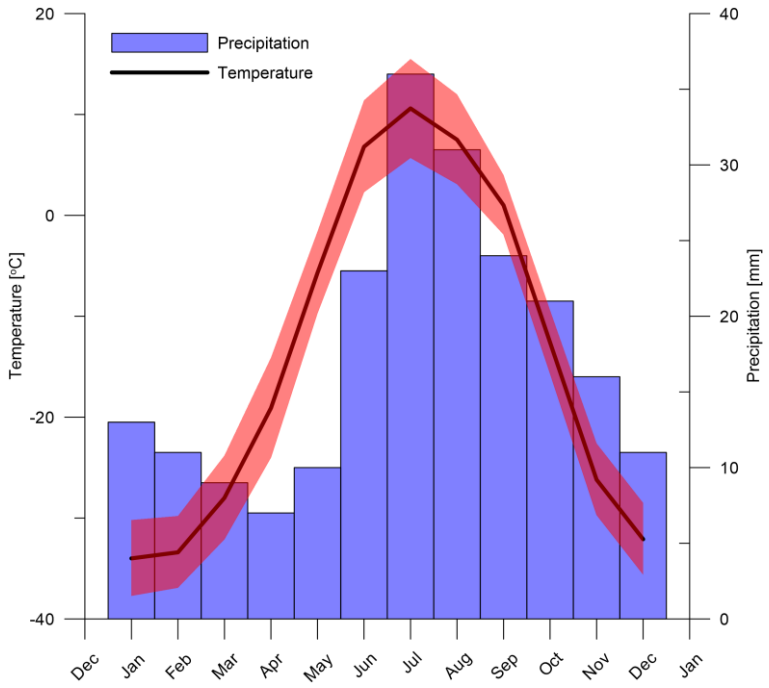

Figure 2. Climate conditions for the city of Chokurdakh (data from "Climate: Chokurdakh", 2016).

The Berelekh River is a west to east oriented river that is strongly meandering between the Allaikhovski Highland in the south and by thermokarst depression (alas plain) with several Yedoma hills in the north (figure 3; Schirrmeister et al., 2012). The depth of the river near the research area fluctuates between 5 and 15 meter. The width of the river depends on the amount of runoff due to the low differences in altitude in the area, but it can extent up to 200 meter. The river is covered by ice between October and May. The stream samples were taken from one of the tributaries of the Berelekh River. This tributary, the Konsor-Syane River, flows north to south through the alas plain (figure 3), and cuts some high pingos, approximately 5 km upstream of where the stream samples were taken (Schirrmeister et al., 2012). The Konsor-Syane River had an estimated average width of about 50 meter. Important notes of the sample locations are given in appendix 1.

The three lakes that were sampled (green dots in figure 1) have a surface area between 0.04 and 0.51 km^2. The depth of the two smaller lakes (L6 to L12) was around two to three meters, whereas depths up to seven meters were measured for the biggest lake (L1 to L5). The ponds (yellow dots in figure 1) are much smaller with areas between 3 and 240 m^2 and depths of 12 to 40 cm (appendix 2). The composition of lakes and ponds is mainly influenced by snowmelt in spring and precipitation and evaporation in summer. During winter, water bodies and their surrounding soils are frozen so that no precipitation or groundwater can infiltrate the freshwater system (Vonk et al., 2015).

With a total surface area of 3 m^2 and a depth of 12 centimetres, P6 was the smallest pond that was sampled. The sample water was darker compared to the other ponds, and there was visibly more organic matter in the samples. Filtering of these P6 samples was very difficult.

Most of the lake sites are surrounded by grasses, although some banks showed clear visible active thermokarst. Samples were taken close to the active thermokarst (L1 and L3), both located at the biggest lake. The thermokarst processes are expected to result in an increase in the input of permafrost material into the lake, including particulate organic carbon (POC) and dissolved organic carbon (DOC). The active thermokarst near site L1 (yellow triangle in figure 3; figure 4) created a smaller pond that was connected to the big lake. Extra samples were taken from this thermokarst pond (samples identified as TK).

Figure 3. Major landscape elements around the Kytalyk station (green triangle), and the location of the active thermokarst sample. Modified after Schirrmeister et al., (2012)

Figure 4. Picture of the active thermokarst location close to L1 (TK in sample 3).

2.2. Sample site measurements

2.2.1. Particulate and dissolved organic carbon (POC and DOC)

Besides the hydrology and topography of the area, the type of permafrost thaw is also important for the composition and amount of carbon that will be released into the freshwater system. Two different types of dynamics can be identified during the release of carbon into the freshwater system; the long-term press and short-term pulse dynamics (Collins et al., 2007; Schuur et al., 2008). An active layer deepening (press disturbance) will most likely result in the supply of soluble material (DOC), where thermokarst erosional features (TEFs; pulse disturbance) are expected to supply mostly particulate organic material (POC) to the system (Vonk et al., 2015). Long term changes in active layer deepening will most likely occur at all sample sites due to anthropogenic climate change, but these changes are very subtle and require long term research before changes can be found. In contrast, TEFs can have intense impact on a local area although they have a shorter time span and occur on a smaller scale. For this research, TEFs were found near two different sample locations (L1 and L3). The TEF near L1 was sampled directly (TK). This sample locations showed clear active thermokarst (figure 4).

2.2.2. Dissolved gas concentrations (CO_2, CH_4, and N_2O)

When permafrost carbon is decomposed, it can be released into the atmosphere as greenhouse gas (CO_2 and CH_4). Most of the decomposed carbon will consist of CO_2, although also methane (CH_4) can be produced if oxygen is limited (such as in saturated soils, ponds, and lakes; Ciais et al., 2013). Increasing temperatures in the Arctic can result in the deepening of the active layer, which is the top soil layer that thaws during the summer. Due to the increase in active layer thickness, and the longer duration of the thaw period, the organic substrate that will be available for microbes will increase. In contrast to that, higher temperatures will also lead to a greater uptake of CO_2 by Arctic vegetation (Ciais et al., 2013). Besides these processes, local hydrological conditions are important for the amount and type of carbon decomposition. The high complexity of these processes increase the difficulty to give a good estimate of (future) carbon fluxes from permafrost systems to the atmosphere.

To get a better understanding of the amount of the different greenhouse gases in Arctic freshwater systems, the most important dissolved gas concentrations (CO_2, CH_4 and N_2O) were measured for the different sample sites. Dissolved gas concentrations for the different water bodies (ponds, lakes, and streams), as well as atmospheric gas concentrations were measured. Vertical fluxes of greenhouse gases were calculated by comparing the amount of greenhouse gases in the sample water to the amount found in the atmosphere, measured by the eddy covariance tower and in the field.

2.2.3. Stable isotopes ($\delta^{18}O$ and $\delta^{2}H$)

Stable isotopes, $\delta^{18}O$ and $\delta^{2}H$, of water samples can be used as a tracer for the hydrologic composition of the different sample sites. As the carbon and hydrologic cycles are closely linked in the Arctic region, the stable isotope composition of the different sample waters for this research can help with analysing the origin and composition of the carbon content. The pond, lake and stream waters may have different $\delta^{18}O$ and $\delta^{2}H$ signatures, which are dependent on the input and output of hydrological components such as groundwater, direct and indirect precipitation, evaporation, and surface and stream outflow and inflow (Jonsson et al., 2009).

By comparing the amount of heavy isotopic species of the water sample ($^{1}H^{2}H^{16}O$ and $^{1}H^{1}H^{18}O$) to the amount of light, more common isotopic species ($^{1}H^{1}H^{16}O$), a ratio between light and heavy isotopes can be achieved (Gibson et al., 1993). These $^{2}H/^{1}H$ and $^{18}O/^{16}O$ ratios are displayed in parts per thousand (‰) relative to the Vienna Standard Mean Ocean Water (VSMOW). Craig (1961) found a linear correlation between $\delta^{18}O$ and $\delta^{2}H$ values of natural terrestrial waters. This correlation (equation 1), known as the Global Meteoric Water Line (GMWL), is based on weighted monthly precipitation data from several hundred of stations all over the world (Gibson and Edwards, 2002).

$$\delta^{2}H = 8 * \delta^{18}O + 10 \quad (1)$$

Regional waters that have not experienced any evaporation, such as direct precipitation, roughly fall along a Local Meteoric Water Line (LMWL). This LMWL is commonly very similar to the GMWL, with a slope close or equal to the slope of the GMWL. Small variations between the LMWL and the GMWL occur due to temperature-dependent effects of the condensation of atmospheric vapour (Gibson et al., 1993).

The isotopic composition of water can be altered, mainly due to evaporation, resulting in a local evaporation line (LEL). This LEL is generally enriched in $\delta^{18}O$ and has a slope normally in the range of 4 to 6, which is much less than the slope of the GMWL and the LMWL (8; Gibson et al., 1993). This slope is primarily influenced by local conditions such as temperature and humidity. Stable isotope conditions of the water bodies are fluctuating over the year, indicating the origin of the water body. Permafrost water bodies that have a LEL with a slope around 6 commonly have a main source of thawed ice, whereas summer precipitation and evapotranspiration are the main source for LELs with slopes around 4 (Gibson et al., 1993). The intersection of the LEL with the LMWL is normally used as the mean isotopic composition of annual precipitation for that area (Gibson et al., 1993).

The relative position of sample data in respect to the GMWL can be visualized by the deuterium excess value (equation 2). A deuterium excess (*d* excess) of 0 equals the composition of average ocean water (VSMOW), where the GMWL has a *d* excess value of 10. This difference between oceanic and GMWL *d* excess values occurs due to the deuterium enrichment of the evaporation of ocean water (Kendall and McDonnell, 2012). Water bodies that are sourced mainly by summer precipitation are likely to have lower *d* excess values and have slightly enriched $\delta^{18}O$ values, as winter precipitation tends to have a more depleted isotopic conditions in relation to summer precipitation (Jonsson et al., 2009).

$$d \text{ excess} = \delta^{2}H - 8 * \delta^{18}O \quad (2)$$

Both $\delta^{18}O$ and $\delta^{2}H$ values were measured for all of the sample locations in order to determine the variability between the different types of freshwater systems. This variability will result in an estimate of the origin of the sample water, and thereby contribute to a better understanding of the source of carbon.

3. Material and methods

3.1. Sample collection

Collection of the samples took place between 31 July 2016 and 10 August 2016. Average temperature during the sampling was 14 degrees, with some rain during the last days of the sampling. A total of 28 different locations were selected for sampling; 12 lake, 12 pond, and 4 stream sites (figure 1). Each location was sampled three times, at an average interval of three days. Appendix 2 gives an overview of the properties of the different sample locations. At each sampling site water temperature, electrical conductivity (EC), and pH were measured. These measurements were taken at approximately 5-10 cm water depth. The timing and results of these measurements can be found in appendix 3. All vials were rinsed three times with sample water prior to the sample collection. The samples were taken roughly 5 to 10 cm below the water surface and as far away of the shore as possible without disturbing the water.

Surface area, depth and active layer thickness of the pond sites was measured after the last sample collections. The average depth of five representative locations approximately 1 meter from the pond side was used for the active layer thickness (appendix 2).

3.1.1. Dissolved gas concentrations

For the measurements of the dissolved gas concentrations, the syringe-headspace technique was used (Teodoru et al., 2009; Abril et al., 2015). A 60 ml syringe, attached to a two-way valve, was filled with a combination of 30 ml of sample water and 30 ml of atmospheric air. The syringe was vigorously shaken during 1 minute to achieve equilibrium between the water and the headspace. The headspace was then transferred to a 30 ml syringe by a two-way valve, after which the gas was injected into a 12 ml pre-evacuated exetainer to achieve slight over-pressure. Every day, a reference ambient air sample was collected in order to obtain the atmospheric CO_2, CH_4, and N_2O concentrations. Besides these ambient air samples, gas concentration data from the eddy covariance tower in the Kytalyk basecamp were used as a reference. The exetainers filled with gas were stored in a dry and dark place until they were analysed at the Chemical Oceanography laboratory of the Université de Liège, Belgium.

Water temperature and electrical conductivity were measured during every sample collection, in order to calculate gas concentrations and fluxes. The data was used to calculate the salinity concentrations (“Standard Methods for the Examination of Water and Wastewater”, 1999). Daily and hourly average wind speed and atmospheric pressure data were obtained from the eddy covariance tower, near the base camp.

3.1.2. POC and DOC

At each sample location 100 ml of sample water was collected for POC and DOC analyses. Due to the occurrence of small organisms at some of the ponds, a fine net was used to filter out these organisms as best as possible to reduce heterogeneity. For all samples, the presence of air bubbles in the vials was minimized in order to reduce the degassing. The samples were stored in a cool and dark place until they were filtered (usually performed on the same day of sample collection) on 0.7µm pore size Whatman GF/F glass fiber filters with a diameter of 47mm, using a Millipore® vacuum filter tower. The filters were air dried indoors and stored in a dry and dark place until they were analysed at the department of Ecological Science, Vrije Universiteit Amsterdam.

The filtrate was used for the DOC measurements. The DOC samples were acidified by adding nitric acid (60% HNO_3) to a pH ~2 in order to limit the microbial activity during transport. The samples were refrigerated at the VU Amsterdam before they were transported and analysed at the department of Earth & Environmental Sciences, University of Leuven, Belgium.

3.1.3. $\delta^{18}O$ and $\delta^{2}H$

The stable isotope samples for $\delta^{18}O$ and $\delta^{2}H$ measurements were collected in 20 ml vials. Degassing of the samples was minimized by keeping the headspace of the sample to a minimum. Stable isotope samples were not obtained for all locations, but for each of the three different water bodies a few representative sites were chosen (appendix 3). After collection and transport, samples were refrigerated before they were analysed at the stable isotope laboratory of the Earth Science department, Vrije Universiteit Amsterdam.

3.2. Sample analyses

3.2.1. Dissolved gas concentrations

The 12 ml gas filled exetainers of all the collected gas samples were measured with gas chromatography (GC) at the Chemical Oceanography laboratory of the Université de Liège, Belgium (figure 5). By using the SRI 8610C Gas Chromatograph, the concentrations of CO_2, CH_4, and N_2O of the 84 samples were determined. The detector was calibrated by measuring three standards with different CO_2:CH_4:N_2O compositions (table 1). These standards were analysed at the start and end of each daily batch of samples.

The collected gas samples were transferred from the exetainer to a syringe via the septum of the exetainer. In order to keep the atmospheric pressure of the exetainer at a constant level, the gas volume was replaced by a saline solution injected via another syringe. The sample was then injected from the syringe into the gas chromatograph. Final concentrations were computed by using the solubility coefficient given by Yamamoto et al. (1976).

Fluxes of the measured concentrations were estimated by using a wind-based equation (Laurion et al., 2010):

$$F = k * \Delta concentration \quad (3)$$

Where k is the gas transfer velocity and $\Delta concentration$ is the difference between the measured sample concentration of CH_4, CO_2, or N_2O and the atmospheric concentration of the different gases. Atmospheric concentrations were measured by the eddy covariance tower and by hand in the field. The value of k is computed based on wind speed, by using the method described by Cole and Caraco (1998), and the Schmidt number, which is based on the water temperature. Wind speed data of the eddy covariance tower was converted to a 10m height wind speed by using the wind profile power law of Johnson et al. (1998):

$$u = u_r * \left(\frac{10}{z_r}\right)^a \quad (4)$$

Where u is the wind speed at a height of 10 meter, and u_r is the wind speed at the height of the eddy covariance tower (z_r or 4.5 meter). The coefficient a is empirically derived, based on the stability of the atmosphere. For this research a value of 0.108 was used for a. Hourly wind speed data were used in this equation. Due to large changes in wind speed during the measurements (between 2.3 and 8.4 m/s) and the distance between the tower and some of the sample locations (> two kilometre), there is an unknown error range in the wind speed factor.

Although fluxes were calculated for all three different water body types, only the fluxes for lake samples are expected to be reliable. For stream and pond fluxes, important parameters are missing in the method of calculating these fluxes. Important parameters as water depth, current, and flow velocity are not incorporated in the flux measurements for the stream sites. These parameters were not available for this research. The impact of wind speed on pond sites is very different compared to lake sites and no commonly-accepted equation exists to give a good estimate for reliable pond fluxes. Where wind turbulence is only affecting the top water layer of the lakes, the wind turbulence on a shallow pond is affecting the entire pond system and thereby also the soil below the pond site. Furthermore, smaller ponds have a smaller fetch, resulting in a reduced mixing zone. Due to the high inaccuracy of the flux data for both ponds and streams, this research mainly focussed on the measured concentrations.

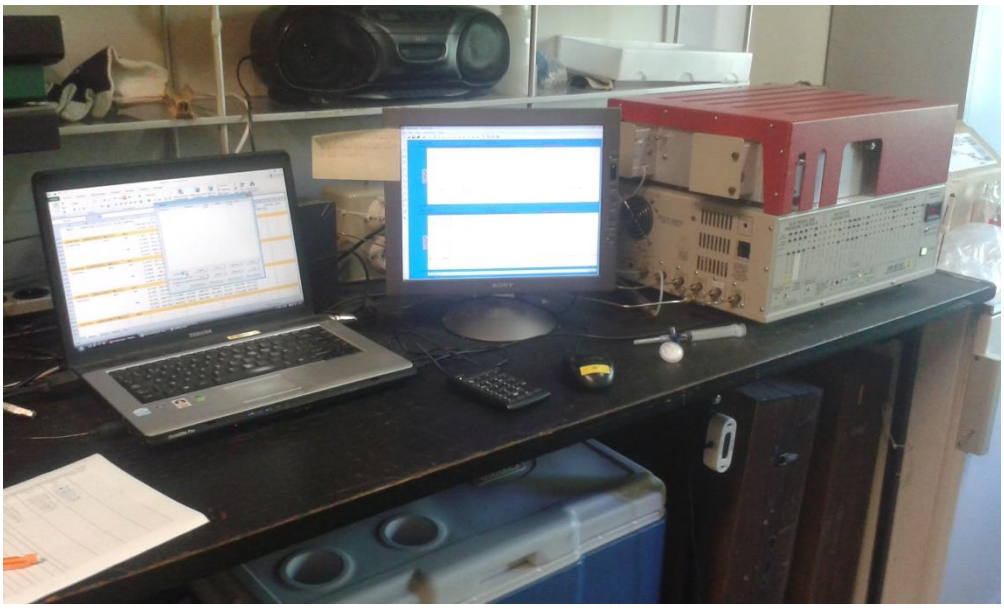

Figure 5. Setup of the dissolved gas concentration measurements in Liège, Belgium. The box with the red top is the flame ionization detector.

	CO_2 (ppmv)	CH_4 (ppmv)	N_2O (ppmv)
Standard 1	400	1	0.2
Standard 2	1000	10	2
Standard 3	4000	30	5

Table 1. Standards and their concentrations used for the gas concentration measurement.

3.2.2. POC

A total of 84 POC filter samples were achieved, including 10 duplicates in order to get a better understanding on the variability of this method. The analyses of the POC filters are based on a modified protocol from the Örjan Gustafsson Lab (Stockholm University), *Organic Carbon of sediment and GF/F filters*. The dried filters were punched with a 4 mm diameter steel punch (figure 6a). A maximum of 16 punched filter pieces, depending on the amount of material on the filter, was transferred to an Ag capsule (5mm diameter; 9 mm high). The Ag capsules were burnt in a beaker at 450°C over night before used. Then, 25µl of distilled water was added to saturate the sample. Thereafter 25 µl of 1 M HCl was added to the capsule. The samples were given at least 30 minutes at room temperature, covered with Al foil, allowing the HCl to penetrate the filter samples. Thereafter, another 50 µl of 1 M HCl was added to the capsules. After another 30 minutes, the capsules were placed in an oven at 60 °C, covered by Al foil, to dry overnight. Hereafter the Ag capsules were closed and folded into an as small and rounded shape as possible. The capsules were then folded into a tin capsule to facilitate the combustion. The samples were analysed on a Thermo Flash elemental analyzer 1112 series at the Vrije Universiteit of Amsterdam (figure 6b). The results were calibrated based on an aspartic acid standard.

Figure 6. A) Example of punched filters, notice the difference in colour of the different filters. B) The Thermo Flash elemental analyzer 1112 series.

3.2.3. DOC

The acidified DOC samples were analysed at the University of Leuven with the method of wet oxidation by using an Aurora 1030W wet oxidation DOC analyser coupled with the Elemental Analyzer-Isotopic Ratio Mass Spectrometer (EA-IRMS). The DOC samples were gradually oxidized and the resulting CO_2 was concentrated and injected into the EA-IRMS. The resulting DOC concentrations were calibrated by using the IAEA-C6 standard. Besides DOC data, also $\delta^{13}C_{DOC}$ data was achieved.

Not all DOC samples were analysed due to instrumental issues. Of all the pond samples, only the P5 to P12 sites were measured. For the lake sites only the L1 to L9 samples were analysed. The stream site samples, similar to the smaller eastern lake (L10 to L12) and the P1 to P4 pond samples, were not available.

3.2.4. $\delta^{18}O$ and $\delta^{2}H$

Selected site samples were analysed for $\delta^{18}O$ and $\delta^{2}H$ by using the Picarro L2140-*I* at the Vrije Universiteit Amsterdam. Samples were injected into a vaporizing unit at high temperature. The resulting vapour was then analysed. All samples were injected seven times, and were corrected using a calibration line based on the Kona Deep standard. The first three injections were carried out in order to rinse the isotopic water analyser, the last four times to measure the samples. Average data of these four measurements was used for this research. Median standard deviation was 0.05‰ for the $\delta^{18}O$ samples and 0.28‰ for the $\delta^{2}H$ samples.

An online isotope precipitation calculator was used to estimate the average stable isotope concentrations of precipitation in the research area (Bowen, 2009). The model used in this calculator is based on detrended interpolation of tens of thousands of measurements (Bowen et al., 2005). The obtained isotopic precipitation concentration is used to validate the developed local evaporation line (LEL).

3.2.5. Correlations and error ranges

Correlations in this research are based on the Pearson product-moment correlation coefficient (PCC). The PCC measures a linear dependence between variable X and Y. Confidence in a correlation is not only determined by the correlation coefficient, but also by the number of pairs of the data (Fenton and Neil, 2012). This correlation significance was analysed by using a *p*-value. The *p*-value represents the probability if the null hypothesis is true. For this research *p*-values smaller than 0.01 were marked as highly significant. Correlations were computed in Excel and Grapher. *P*-values are computed by using an online converter (Lenhard and Lenhard, 2014).

Error ranges are given in one standard deviation. Correlations and error ranges are based on all individual sample results, except if mentioned otherwise in the report. For some correlations and error ranges outliers are removed.

4. Results

4.1. Dissolved gas concentrations

Figure 7, 8, and 9 show box-Whisker plots with the results of the CO_2, CH_4 and N_2O measurements. The three different water bodies were grouped, although P6 was neglected in the figures as concentrations were extremely high and decreased the visibility of the graphs. The S1 samples showed carbon concentrations similar to the pond samples, and was therefore not incorporated in the stream dataset (appendix 1).

The median CO_2 concentration values for ponds, streams, and lakes are respectively 0.18 ± 0.12, 0.04 ± 0.014 and 0.02 ± 0.005 mg C L^{-1} (error ranges are one standard deviation). For CH_4 these median concentrations are 0.11 ± 0.44, 0.02 ± 0.011 and 0.02 ± 0.005 mg C L^{-1}, and for N_2O the concentrations are 0.05 ± 0.026, 0.09 ± 0.008 and 0.10 ± 0.008 µg N L^{-1}. Ponds show more variability compared to lake and stream concentrations. The highest CO_2 and CH_4 concentrations were found for sample location P6 (mean of respectively: 0.51 and 1.26 mg C L^{-1}). Lowest pond sample gas concentrations were found for the samples P2, P3, and P4, all with values around 0.05 mg C L^{-1} for both CO_2 and CH_4. Furthermore, high CH_4 values were found for sample P10, although this site had average CO_2 concentrations.

The L3 samples showed higher CO_2 concentrations (mean: 0.031 mg C L^{-1}) compared to other lake samples. Other lake samples had consistent CO_2 concentrations (between 0.011 and 0.020 mg C L^{-1}). L3 is one of the sample sites that is located close to the active thermokarst. The L1 samples, close to the TK sample site, only show a small increase in CO_2 concentrations (average 0.019 mg C L^{-1}). The CH_4 concentration of L1 and L3 samples are slightly above average, although within one standard deviation. No dissolved gas concentrations were obtained of the TK sample site.

Compared to the CO_2 and CH_4 concentrations, the N_2O concentrations show an opposite pattern for the three different water bodies. Higher concentrations are found for lake and stream sites and lower concentrations for pond sites. The highest N_2O pond site concentrations were found for P2, P3, and P4, where lowest conditions were found for P10. This is also an opposite pattern as the CO_2 and CH_4 concentrations for pond sites.

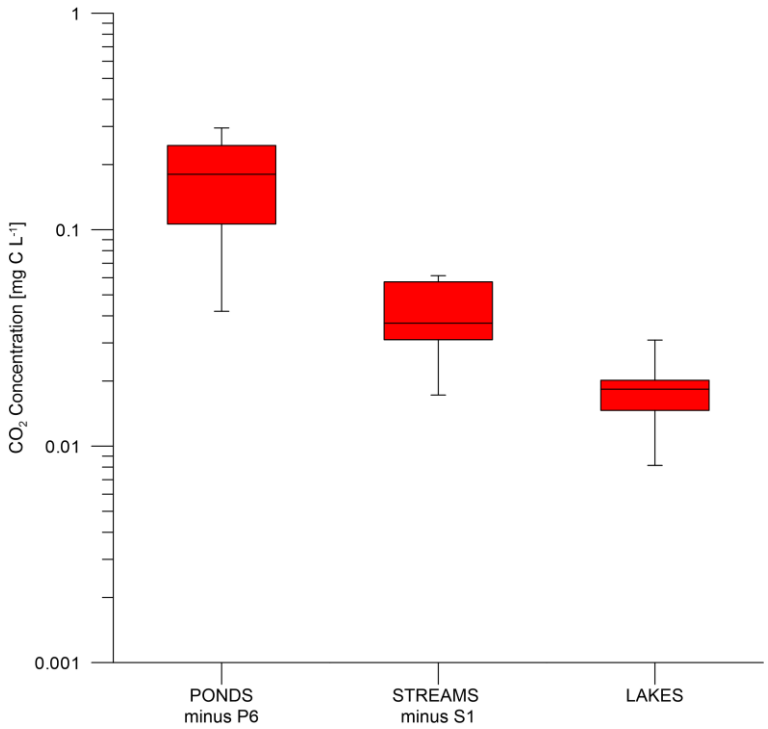

Figure 7. Box-Whisker plot of the CO_2 concentration for ponds, streams and lakes. For the pond sites, P6 was excluded, as well as S1 for the stream sites. Note: the concentration axis is given in a logarithmic scale.

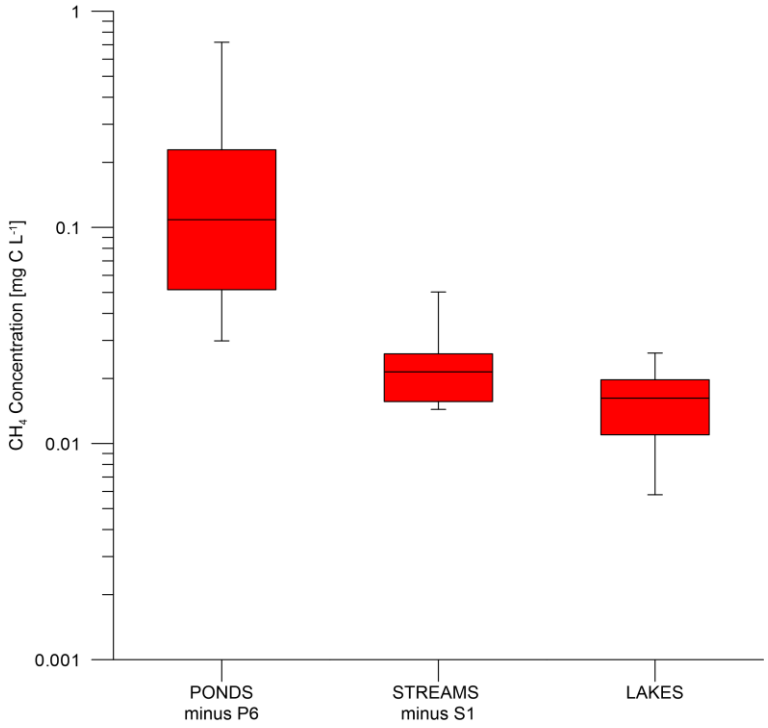

Figure 8. Box-Whisker plot of the CH_4 concentrations for ponds, streams and lakes. For the pond sites, P6 was excluded, as well as S1 for the stream sites. Note: the concentration axis is given in a logarithmic scale.

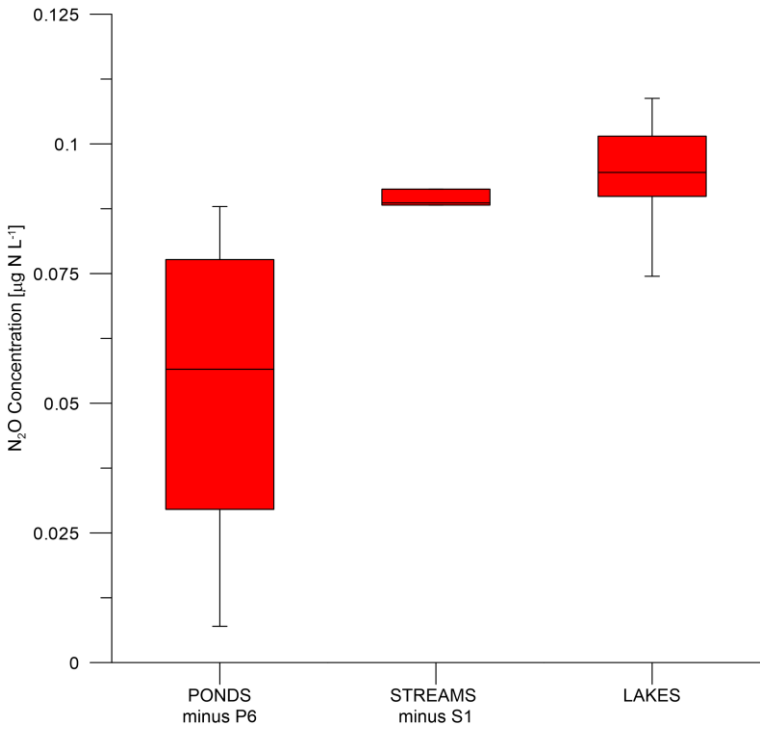

Figure 9. Box-Whisker plot of the N_2O concentrations for ponds, streams and lakes. For the pond sites, P6 was excluded, as well as S1 for the stream sites. Note: in contrast to the CO_2 and CH_4 figures, the concentration axis has a linear scale and the concentrations are displayed as µg N L^{-1}.

4.2. POC

The results of the POC measurements for the three different freshwater systems are displayed in a box-Whisker plot in figure 10. Median POC concentrations for respectively ponds, lakes and streams are 2.44 ± 3.63, 1.09 ± 2.29, and 0.86 ± 1.06 mg C L^{-1}.

Pond samples show some extreme outliers, including the P6 site (mean: 8.26 mg C L^{-1}), P1 (3.50 mg C L^{-1}), P11 (3.22 mg C L^{-1}), and P10 (10.14 mg C L^{-1}). Lowest values were found for sample P8 (1.14 mg C L^{-1}).

The lake POC median site values are in a much smaller range, fluctuating between 0.81 mg C L^{-1} (L5) and 3.01 mg C L^{-1} (L8). As the sites L1 and L3 are located close to visible active thermokarst, the POC concentrations of these sites are of special interest. The L1 site shows a mean concentration of 1.14 mg C L^{-1}, which is nearly equal to the total lake median. The L3 site has a mean concentration well above the total median (2.50 mg C L^{-1}). Furthermore, some of the individual L1 and L3 sample concentrations show extreme outliers (6.37 mg C L^{-1} for L1 and 13.6 mg C L^{-1} for L3).

The POC concentrations for stream sites are fluctuating between 0.62 (S2) and 3.43 (S4) mg C L^{-1}, but show a low median value, even for each individual site. The mean S1 sample POC concentration was similar to median of all pond samples (2.20 to 2.44 mg C L^{-1}).

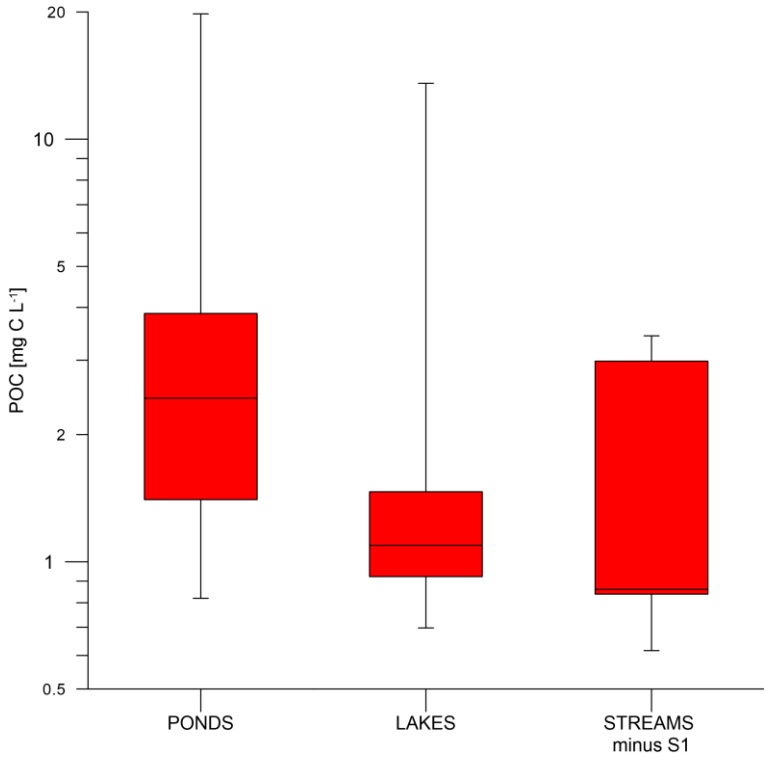

Figure 10. Box-Whisker plot of the particulate organic carbon (POC) concentrations in mg C L^{-1} for ponds, lakes and streams. The S1 site was excluded due to the different conditions compared to the other stream sites. POC concentrations are displayed on a logarithmic scale in order to increase the visibility.

4.3. DOC

The results of the dissolved organic carbon measurements are given in the Box-Whisker plot of figure 11. Due to instrument issues, no DOC data was available for the stream sites. Only data for the P5 to P12 sites was analysed for the ponds, and for the lakes data was obtained for the biggest and western smaller lake (L1 to L9).

The median DOC value for the pond sites is 20.8 ± 12.0 mg C L^{-1}, with minimum and maximum values of 9.3 mg C L^{-1} (P8) and 51.1 mg C L^{-1} (P10). Although the DOC values for the individual sites are quite constant, there is a lot of variation between the different ponds. Site P6, P10, P11 and P12 show values well above the total median, where the other sites show values slightly below total median.

The DOC values of the lake samples vary between 5.0 mg C L^{-1} (L3) and 9.7 mg C L^{-1} (L7), with a median of 7.4 ± 1.49 mg C L^{-1}. Although the variation is much smaller compared to the variation in pond samples, a difference was found between the two measured lakes. The big lake (L1-L5) shows slightly lower values compared to the western small lake (L6-L9). The lower values of the big lake mainly occur due to low concentrations for the L3 samples, one of the samples located close to the active thermokarst.

Besides DOC, also the $\delta^{13}C$ concentrations were measured (figure 12). The fluctuation of pond $\delta^{13}C_{DOC}$ values is higher compared to lake $\delta^{13}C_{DOC}$ values. Highest values were obtained for P6 (-26.53‰) and lowest values for P7 (-28.95‰). No highly significant correlations were found between the $\delta^{13}C_{DOC}$ values and the measured field parameters.

There is a difference in median $\delta^{13}C_{DOC}$ value between both measured lakes (-27.21‰ for the big lake and -27.64‰ for the smaller western lake). No explanation was found for this difference, although the $\delta^{13}C_{DOC}$ values do not seem to be influenced by the active thermokarst at the big lake.

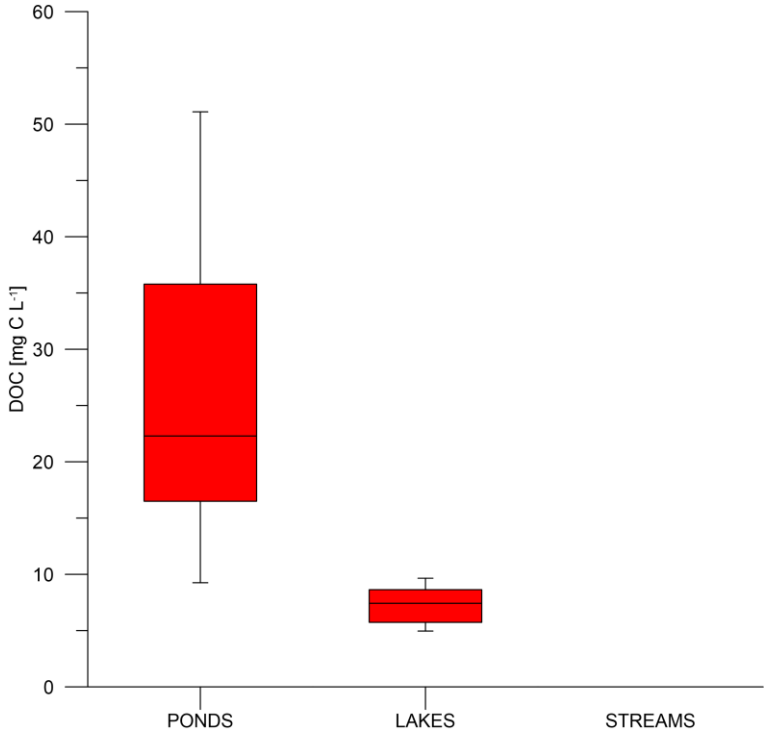

Figure 11. Box-Whisker plot of the dissolved organic carbon (DOC) concentrations in mg C L^{-1} for ponds and lakes. No data for stream sites were available. Not all pond and lake site samples were available for DOC data.

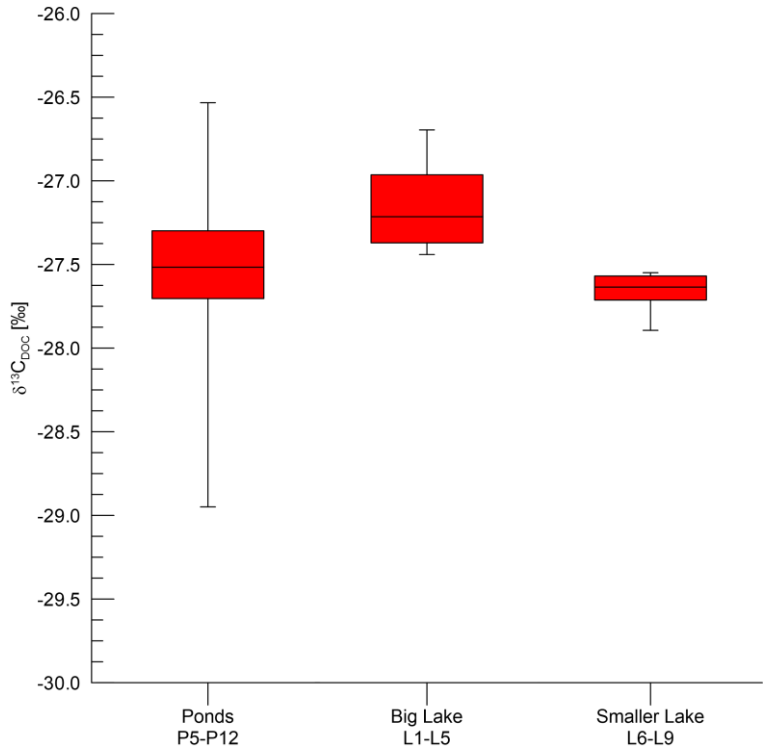

Figure 12. Box-Whisker plot of the $\delta^{13}C_{DOC}$ for both lakes and the ponds. No data for stream sites was available. Not all pond and lake sites samples were available for $\delta^{13}C_{DOC}$ data.

4.4. Stable water isotopes

Figure 13 shows a graph of $\delta^{18}O$ and $\delta^{2}H$ values of all sample locations. The different sites are clustered based on comparable values and similar conditions. Both axes show the $\delta^{18}O$ and $\delta^{2}H$ values in ‰ relative to VSMOW. The thermokarst sample (green triangle in the top box of figure 13), collected at the pond created by the active thermokarst close to sample site L1, plots very close to the GMWL. The other samples show a small offset with less negative $\delta^{18}O$ values.

All lake samples (circles in figure 13) show concentrations for $\delta^{18}O$ and $\delta^{2}H$ along a linear line. The conditions are not similar for the different lakes, as the western small lake (red circles) show less depleted $\delta^{18}O$ and $\delta^{2}H$ concentrations compared to the other lake values. Total mean lake $\delta^{18}O$ and $\delta^{2}H$ concentrations are respectively -16.7 ± 0.33 ‰ and -137 ± 2.3 ‰, with a *d* excess value of -3.41 ± 1.18.

The five measured pond sites (yellow diamond shape) group very well together, while they have completely different values compared to the lake samples. Pond samples show higher, less negative $\delta^{18}O$ and $\delta^{2}H$ concentrations (median of -14.6 ± 0.38 ‰ for $\delta^{18}O$ and -126 ± 2.2 ‰ for $\delta^{2}H$). Furthermore the *d* excess values of the pond sites is more negative (-9.90 ± 2.09). The only exception of the differences between ponds and lakes are the P8 samples. The mean $\delta^{18}O$ and $\delta^{2}H$ values of this site (-16.6‰ and -139‰) are very similar to the lake samples.

No clear correlation was found for the $\delta^{18}O$ and $\delta^{2}H$ composition of the stream sites. An important remark is that there are only two stream sites measured, of which the S1 site is a pond that is most likely connected to the mainstream during high water levels. Still, this pond-like S1 site (-17.3‰ for $\delta^{18}O$ and -139‰ for $\delta^{2}H$) show very similar $\delta^{18}O$ and $\delta^{2}H$ conditions to lake samples instead of the expected pond samples. The concentrations of the regular S3 stream site are more similar to the pond sites with $\delta^{18}O$ and $\delta^{2}H$ values of -15.2‰ and -127‰, although the *d* excess of the S3 site is less negative (-5.83 ± 1.1 ‰).

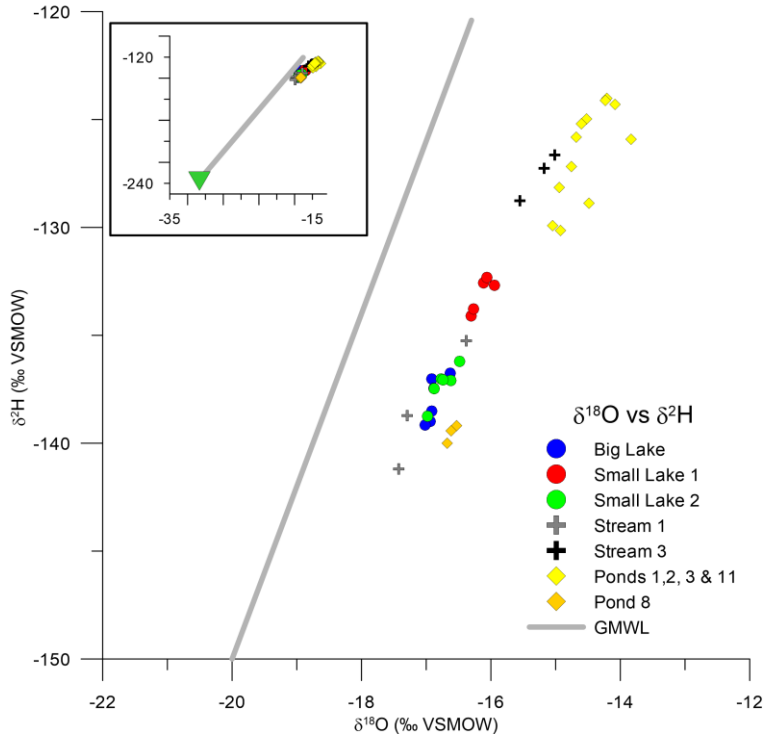

Figure 13. Graph of the $\delta^{18}O$ and $\delta^{2}H$ measurements. Samples with comparing concentrations and conditions were clustered by using various symbols. In the upper left box, the green triangle is displaying the location of the thermokarst sample compared to the other samples. The grey line represents the Global Meteoric Water Line.

5. Discussion

5.1. Dissolved gas concentrations and fluxes

5.1.1. Concentrations

Dissolved gas concentration data achieved for this research were compared to data measured by Goovaerts (2016) (table 2). Goovaerts (2016) measured dissolved gas concentrations in the same area during a fieldwork in the summer of 2015. Comparable ponds, lakes, and streams samples in the Kytalyk research area were obtained, although the exact location of the sample sites is not similar. Concentrations displayed in this table are the median values of the available data. Most of the concentrations fall within the error range of one standard deviation. Lake CO_2 concentrations are lower compared to the previous research, whereas CH_4 concentrations are increased. Due to the high error range for streams and ponds, no conclusion can be obtained from these concentrations. A slight decrease in N_2O is visible for the lake and stream concentrations.

	CO_2 (mg C L^{-1})		CH_4 (mg C L^{-1})		N_2O (µg N L^{-1})	
	1	**2**	**1**	**2**	**1**	**2**
Ponds	0.090	0.175 ± 0.124	0.063	0.112 ± 0.445	0.083	0.066 ± 0.026
Lakes	0.027	0.019 ± 0.005	0.007	0.016 ± 0.005	0.110	0.095 ± 0.008
Streams	0.030	0.037 ± 0.014	0.010	0.019 ± 0.011	0.114	0.091 ± 0.008

Table 2. Data of Goovaerts (2016) (as number 1) and from this research (as number 2) of the different gas concentrations in mg C L^{-1}. Error ranges are one standard deviation. Note that the N_2O data is displayed in µg N L^{-1}.

The CO_2 concentrations of this research are comparable or slightly higher compared to CH_4 concentrations. Pond gas concentrations are on average 8 times higher for both CH_4 and CO_2 compared to the lake site concentrations. Especially for CO_2, this is a major increase in ratio compared to previous data of this research area.

As CO_2 and CH_4 concentrations in this research are very similar and the warming potential of CH_4 is about 25 times higher compared to atmospheric CO_2, the impact of potential CH_4 release in permafrost regions can have a major impact on the global warming potential. Atmospheric N_2O greenhouse warming potential is even higher then CH_4, although the N_2O concentration measured in the water samples is much smaller.

Pond sites, although they have a much smaller surface area and water depth, have much higher gas concentrations and could potentially be of significant importance for future carbon emission in permafrost regions.

5.1.2. Fluxes

Flux data was measured based on the research of Cole and Caraco (1998). The gas transfer coefficient, or *k* value (table 3), controlls the rate of gas exchange between the freshwater system and the atmosphere together with the concentration gradient (equation 3). Although fluxes for lake sites are expected to be quite reliable, this is not expected for the pond and stream sites. Important parameters such as depth, discharge and gradient of the water are not incorparated in the measurements for stream fluxes, although they are most likely an important factor in the gas transfer coefficient (Alin et al., 2011). The *k* value of different stream research in Arctic area show a broad range of values between 3 and 61 cm h^{-1} (Denfeld et al., 2013; Ran et al., 2015; Alin et al., 2011), obtained by using different equations. The high uncertainty of this *k* value for stream sites makes the flux data for this research highly debatable.

Similarly, the flux data of the pond sites is highly uncertain. Ponds in the research area are very shallow (on the order of a few decimeters), and therefore will likely have a totally different interaction with the atmosphere compared to lakes. Turbulence occuring due to wind conditions, which is an important factor for the *k* value, will not have a consistent influence on the total pond area. For lake sites, the turbulence will only affect the top water layer. Although there are differences between ponds, lakes, and streams, the *k* values of this research are based on the same equation due to the lack in better information for pond and stream concentrations.

CO_2	Ponds	Streams	Lakes	CH_4	Ponds	Streams	Lakes
Average	10.8	8.0	6.9	**Average**	6.4	5.2	4.9
Median	13.0	7.6	6.1	**Median**	7.3	5.1	4.5

Table 3. K values for the CO_2 and CH_4 fluxes in this study. K values are based on the equation of Cole and Caraco (1998).

Because of the high uncertainty of the pond and stream flux data, fluxes are only reported for the three different lakes. Calculated CO_2 and CH_4 fluxes are presented in figure 14. Fluxes of the two smaller lakes are very similar to each other (western lake: 42.2 ± 15.6 mmol m^{-2} d^{-1} for CO_2 and 1.15 ± 0.59 mmol m^{-2} d^{-1} for CH_4; eastern lake: 41.5 ± 8.7 mmol m^{-2} d^{-1} for CO_2 and 1.70 ± 0.33 mmol m^{-2} d^{-1} for CH_4). The CO_2 fluxes for the bigger lake are much more diverse compared to the other two lakes (bigger lake: 22.6 ± 29.6 mmol m^{-2} d^{-1} for CO_2 and 1.75 ± 0.54 mmol m^{-2} d^{-1} for CH_4). One of the samples shows even a negative flux for CO_2 (L5), although values more than 100 mmol m^{-2} d^{-1} were also calculated. The four samples with values above 50 mmol m^{-2} d^{-1} are all from the L1 and L3 sites. These are the sites close to the active thermokarst. This possible impact of active thermokarst on CO_2 fluxes is not found for the CH_4 fluxes, as no increase in CH_4 flux was found for any of the L1 and L3 samples. The CH_4 fluxes are relatively constant for all the different lake samples.

Although the biggest lake shows some high CO_2 outliers near active thermokarst, the median flux in CO_2 is much lower compared to the two smaller lakes (22.6 versus 42.2 and 41.5 mmol m^{-2} d^{-1}). The active thermokarst at part of the biggest lake is not resulting in higher CO_2 and CH_4 concentrations and fluxes for the entire lake. Higher concentrations of pH and conductivity were found in the biggest lake. These high concentrations were not found for the two smaller lakes. No explanation was found for the clear pH and conductivity differences between the different lakes.

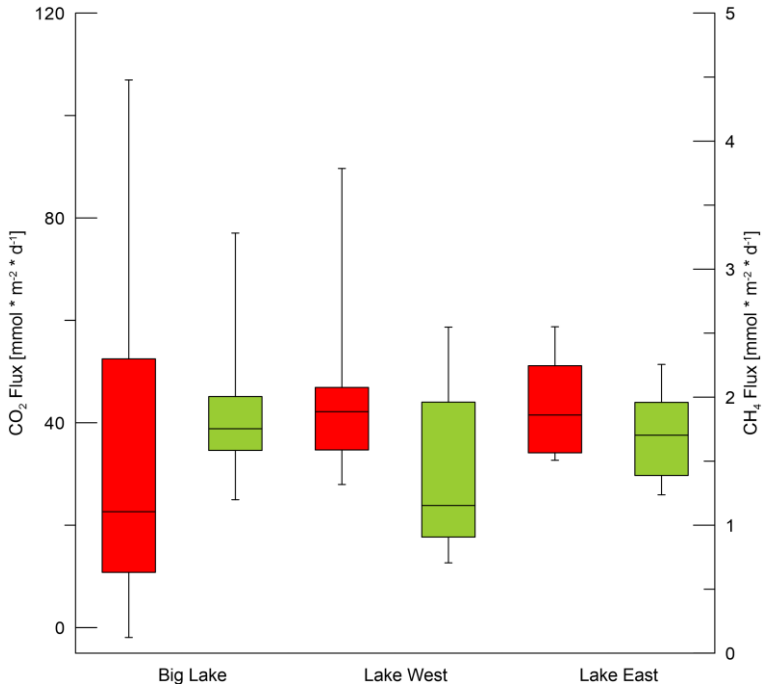

Figure 14. Box-Whisker plot of the CO_2 (red) and CH_4 (green) fluxes for the three different lakes measured during this research. Fluxes are based on the equation of Cole and Caraco (1998). The CH_4 fluxes are plotted on a different y-axis.

5.1.3. Comparison with Arctic dissolved gas concentration and flux measurements

There exists a high variability in dissolved gas fluxes within different Arctic lake researches (table 4). If the data is compared to data of the same research area (this research versus Goovaerts, 2016), fluxes are slightly lower, although they are within one standard deviation. The flux differences between this data and the data of other research can likely be attributed to different calculations of the gas transfer velocity. A possible reason for the inaccuracy of the *k* value can be the impact of the wind speed factor. The wind speed is really important for the *k* value in the equation of Cole and Caraco (1998). For this research average hourly wind speed data was used, obtained by the local eddy covariance tower. Still, wind speed fluctuated a lot over time, and the lakes were kilometres away from the tower location, so that even the local wind speed data are not sufficiently accurate.

	Location	CO_2 [mmol m^{-2} d^{-1}]	CH_4 [mmol m^{-2} d^{-1}]
This research	Kytalyk, Russia	40.2 ± 21.7	1.66 ± 0.5
Goovaerts, 2016	Kytalyk, Russia[1]	66.9	1.83
Wik et al., 2016	Various; north of 50˚N		0.78
Kling et al., 1992a	North Slope, Alaska	17.8 ± 16.6	0.32 ± 0.26
Holgerson & Raymond, 2016	Various global lakes[2]	85.2 ± 8.9	0.42 ± 0.14

Table 4. Calculated CO_2 and CH_4 flux data for lake waters. Data of this research is compared to flux data of other Arctic research. Error ranges are one standard deviation. [1]Data of Goovaerts (2016) is not of exactly the same samples sites. [2]Not only for permafrost regions, but global lake fluxes.

Due to the high uncertainty in the flux data, this report mainly focusses on the concentration data of the different forms of carbon. To increase the reliability of the flux data, a better understanding in the

impact of the wind speed factor on these fluxes is needed. Separate equations are needed in order to measure reliable fluxes for ponds and streams. These equations should include more parameters such as discharge, gradient, and water depth.

5.2. POC

Similar to the gas concentrations, the POC concentrations of the three different water bodies show very different values. The highest POC concentrations are found for the pond sites. These high POC conditions for pond sites in respect to lake sites were expected as ponds have a relatively high exposed soil surface area relative to their volume, so that more interaction can take place between the water and the soil. If the data of POC concentrations is compared to the surface area of the water body (figure 15), a clear negative correlation is visible (power fit; r=0.66; n=91). Water bodies with a larger surface area have significant lower POC concentrations. This correlation is not only found for the different water types, but also within the different pond sites (power fit; r=0.69; n=43).

Although mean L1 and L3 POC concentrations are just above the total lake median (1.14 mg C L^{-1} and 2.50 mg C L^{-1} versus 1.09 mg C L^{-1}), both sites show extreme outliers (6.37 mg C L^{-1} for L1 and 13.6 mg C L^{-1} for L3). As these extreme concentrations are not found at any of the other lake samples, they are most likely caused by the nearby active thermokarst. Due to the high outliers of the L1 and L3 samples, all concentrations for these two sites are excluded in the correlation. No correlation was found between any of these high POC concentrations and the measured field parameters.

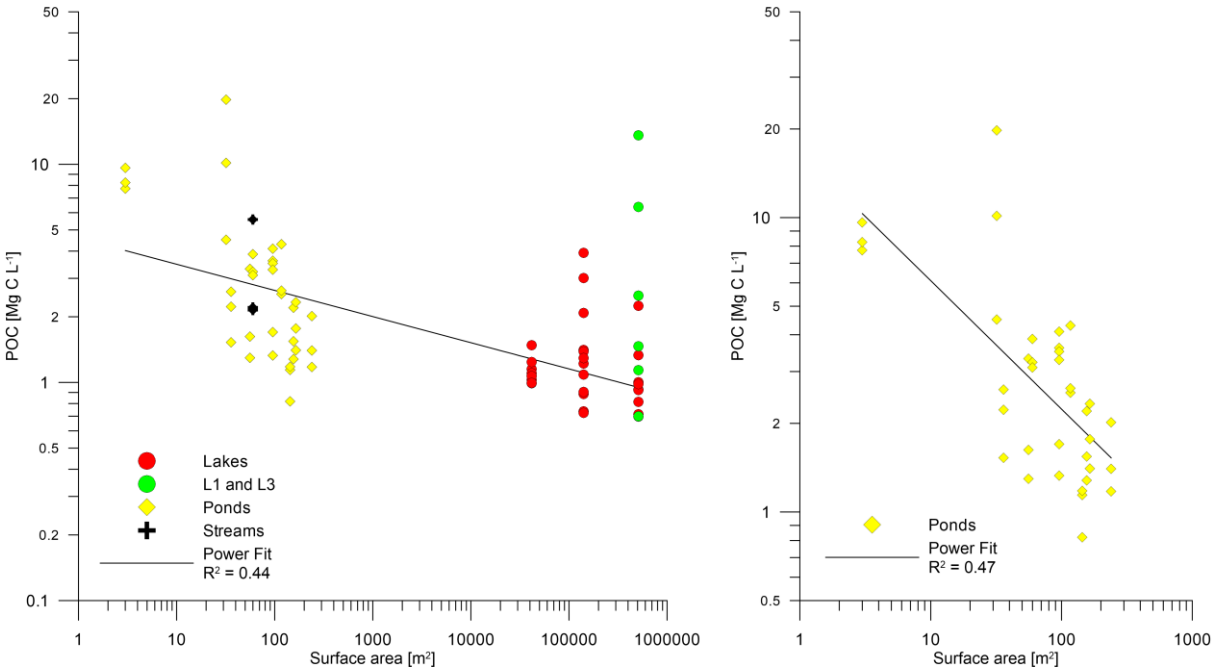

Figure 15. POC concentrations versus the surface area of the water body. 14a shows all available samples (n=91), 14b only displays the pond samples (n=43). Both axes are on a logarithmic scale. Excluded for the trend line are the L1 and L3 samples (green circles).

5.2.1. Comparison with Arctic POC measurements

Although there is a large standard deviation for the POC measurements, a clear difference is found between pond and lake concentrations. The median POC concentration of pond sites is three times higher compared to the median lake concentration. This difference is not found in any other Arctic region POC research (table 5). It should be noted that there is little research that measured POC for both ponds and lakes in the same system. The stream data of this research is slightly lower compared to other research. Most other research was carried out in broader streams with higher flow rate so that particles will settle less easily.

POC [mg C L^{-1}]	Location	Ponds	Streams	Lakes
This research	Kytalyk, Russia	2.43 ± 3.63	0.86 ± 1.06	1.09 ± 2.29
Goovaerts, 2016	Kytalyk, Russia	1.26 ± 0.79	1.10 ± 0.46	1.18 ± 1.68
Lim and Douglas, 2003	Devon Island, Canada	0.32 ± 0.18		0.25 ± 0.05
Guo et al., 2007	Sagavanirktok, Alaska		1.26 ± 0.90	

Table 5. Median concentrations of POC for different research in the Arctic region.

The clear correlation between POC concentrations and surface area indicates a higher potential DOC and CO_2 production for smaller ponds compared to bigger lakes (Goulsbra et al., 2016). Due to the small depth of the different ponds, it is most likely that high POC concentrations are caused by the resuspension of particles. This constant resuspension of settled material caused by wind turbulence can extend the exposure time of POC and thereby increase the potential for degradation of organic carbon in ponds. The significantly lower POC concentrations in the lake sample of this research suggest a smaller exposure time. As POC material is exposed for a shorter time interval, large lake sites have a higher potential for settling and burial of the material.

5.2.2. Limitation of the POC measurements

Despite thorough testing and the use of blanks and standards, the POC method that was used introduces a fairly high variability. Material on the filter is heterogeneously distributed, and punching random “representative” holes for OC analyses will unavoidably introduce errors. Due to the absence of enough material, it was not possible to duplicate all the samples. The duplicates that were measured (n=10) show a median error of 18%.

As particles tend to settle rapidly, especially in lakes, the exposure time of the POC is very important for the measured concentrations. For this exposure time, the particle size is a critical parameter. Although this particle size is not measured, it is expected to be very small. The minimum size of a POC particle is 0.7µm.

The small organisms, mainly found in the pond sites, can have an important impact on the carbon measurements. Although POC samples were filtered as soon as possible after they were collected, and the small organisms were filtered out as well as possible, their impact remains uncertain. In order to decrease this uncertainty, a better sampling technique is needed for future POC measurements in the Arctic region, for instant by using a coarse pre-filter that performs better than the simple net that was used.

5.3. DOC

DOC data was not available for all sites. Still, the available data was compared to data from other research in the Arctic region (table 6). The DOC concentrations in other Arctic regions shows a very broad range of concentrations. Pond site DOC concentrations are significantly higher compared to the lake site concentrations, although they also show a higher variability. Similar to POC data, the size and depth of the freshwater system are very important for the amount of DOC.

DOC [mg C L^{-1}]	Location	Ponds	Streams	Lakes
This research	Kytalyk, Russia	20.8 ± 12.0		7.4 ± 1.5
Goovaerts, 2016	Kytalyk, Russia	19.6 ± 5.3	11.2 ± 5.6	11.6 ± 2.7
Lim and Douglas, 2003	Devon Island, Canada	1.9 ± 1.6		1.7 ± 0.8
Guo et al., 2007	Sagavanirktok, Alaska		1.1 ± 0.5	
Abnizova et al., 2012	Samoylov Island, Russia	5.8		3.3
Dean et al., 2016	Northwest Territories, Canada	32.6 ± 1.0	23.0 ± 0.6	16.6 ± 0.7

Table 6. Median concentrations of DOC for different research in the Arctic region.

5.4. Stable isotopes

Where most of the ponds show very different stable isotope values compared to the lake samples, this is not the case for the P8 samples. Although the conditions of this pond (size, depth, and carbon concentrations) are very similar to the other pond sites, their stable isotope measurements plot more closely to the lake samples. Of all measured field parameters, the only clear difference that was found between the P8 samples and the other pond samples was the aluminium content, measured with ICP-MS. The P8 Al concentrations (33.68 ± 0.8 µg/l; n=3) was significantly lower compared to the mean pond concentration (104.85 ± 44.8 µg/l; n=12). Aluminium concentrations of the P8 samples are similar to lake (28.46 ± 16.45 µg/l; n=8) and stream (31.13 ± 12.61 µg/l; n=3) Al concentrations.

Mineral weathering of terrestrial material during high acid conditions results in the formation of aluminium (Driscoll and Schecher, 1990). This Al can be transferred to freshwater systems. High Al concentrations are thought to alter the availability and cyclicity of organic carbon in the freshwater system due to adsorption and coagulation reactions (Driscoll and Schecher, 1990). As the Al content of soils is normally quite high (Shacklette and Boerngen, 1984), the low amount of Al in the P8 sample can be caused by less interaction of the water with the surrounding soil.

Freshwater bodies normally show a negative correlation between Al concentrations and the pH of the water (Driscoll and Schecher, 1990). A low pH increases the solubility of Al. Although P8 aluminium concentrations are lower compared to the other pond sites, the pH of the P8 site show values similar to the other pond sites. The theory of less interaction of the P8 water with the surrounding soil is not strengthened by any of the other parameters.

Slopes of regression between $\delta^{18}O$ and $\delta^{2}H$ for lake samples (6.28) and pond samples (4.29) indicate a difference in the main water source for both systems. Most likely, lakes are mainly influenced by thawed ice from ice wedges in the soil, whereas the ponds are primarily affected by summer precipitation and evapotranspiration (Abnizova et al., 2012). This theory is enhanced by the *d* excess values of lakes (-3.41) and ponds (-9.14), where the much more negative pond samples show a higher impact caused by rain rather than snow. The negative *d* excess value for pond sites are most likely caused by the secondary evaporation of the pond water.

For this research the GMWL was used to compare the data instead of a local meteoric water line (LMWL) due to the lack of reliable local precipitation data. It is expected the LMWL is located close to the GMWL with a similar slope.

5.4.1. Comparing stable isotopes

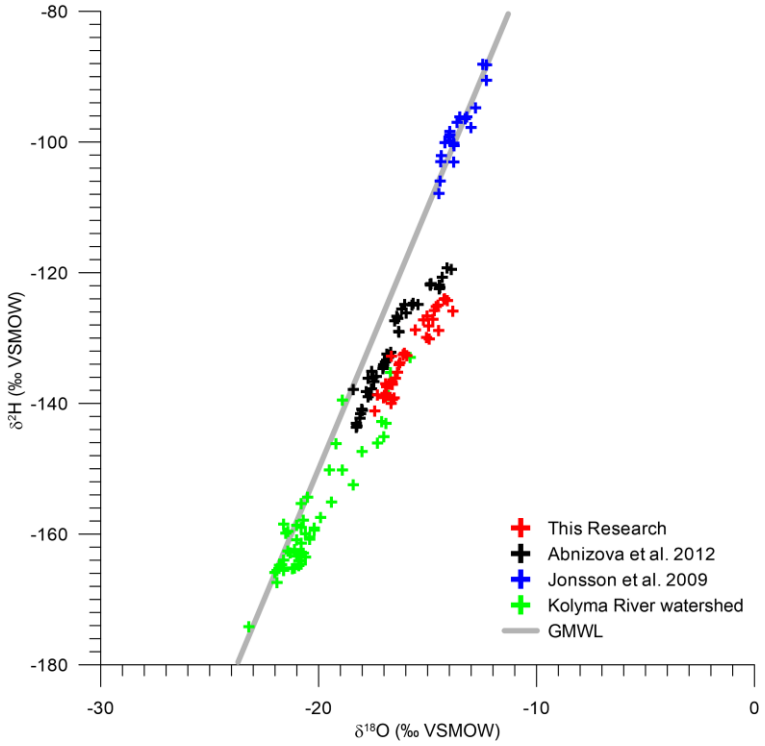

Figure 16. Stable isotope measurements of this research (red) compared to the data of other Arctic stable isotope research.

Figure 16 shows the $\delta^{18}O$ and $\delta^{2}H$ data of different Arctic research. All these data points are closely correlated to the GMWL, although most samples are slightly enriched in $\delta^{18}O$. The *d* excess of this research is on average somewhat more negative, resulting in a larger difference with the GMWL. This difference is mainly caused by the high ratio of pond samples in this research. Other Arctic stable isotope research is mainly focussed on stream and lake samples that are less affected by evaporation.

The Kolyma River watershed data is unpublished data (from Vonk et al.) of 8 lake samples and 31 stream and tributary samples of the Kolyma River, Russia. This research area is located 500 km east of the Kytalyk research area. Isotope data of Abnizova et al. (2012) were obtained from lake, pond, and flood plain water samples from Samoylov Island, a small island in the Lena Delta, 1000 km west of the Kytalyk research area. The 21 samples of Jonsson et al. (2009) are obtained in sub-Arctic lake waters from northern Sweden. The difference in stable isotope ratio between the samples of Jonsson et al. (2009) and the other research is caused by the difference in sample location and the resulting differences in climate conditions.

The results of this research look very similar to the data of Abnizova et al. (2012). This is the only dataset that combines all lake, stream and pond data, similar to this research. Conditions for both sample locations are most likely similar, although samples of Abnizova et al. (2012) are closer located to the Arctic Ocean and the major mainstream.

5.4.2. Local evaporation line

By combining stable isotope data of this research and data from other Siberian research (Abnizova et al., 2012 and Kolyma River watershed data), a local evaporation line (LEL) was created (figure 17). This LEL is closely related to the GMWL, although small differences occur due to local conditions such as temperature and humidity. Also seasonality differences are likely to be found along the line. The LEL is created based on lake and pond samples (n=133).

The intersection of the LEL with the GMWL can be used as the expected mean isotopic annual precipitation composition in the research area (Gibson et al., 1993). For this research, the intersection was found at a $\delta^{18}O$ of -21.3‰ and a $\delta^{2}H$ of -160.6‰ VSMOW. The created LEL has a slope of 5.5, similar to the expected slope between 4 and 6 (Gibson et al., 1993).

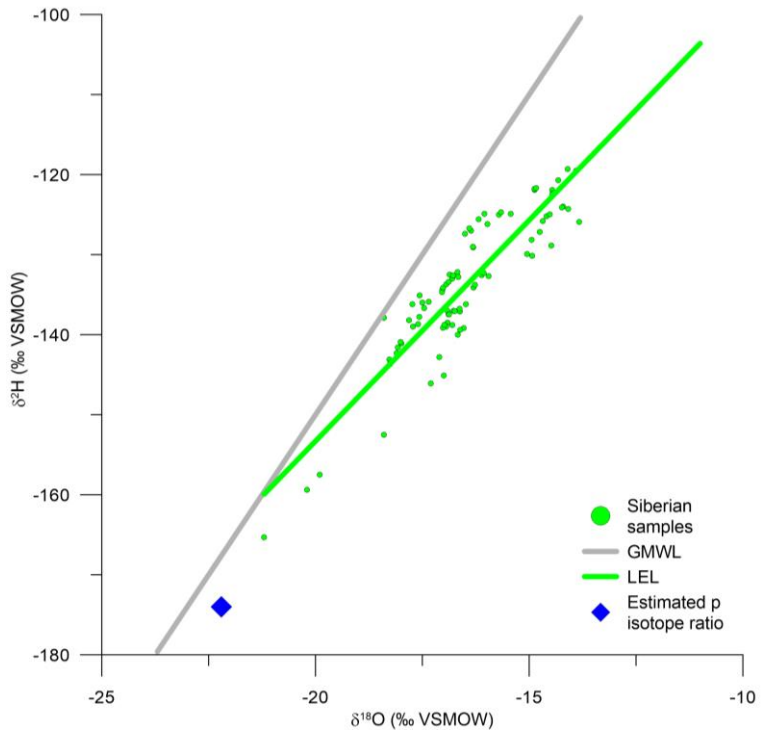

Figure 17. Local evaporation line (LEL) based on different stable isotope datasets in northeast Siberia.

The online isotope precipitation calculator, based on interpolation of tens of thousands of global measurements, estimates a δ^2H value of -174‰ and a $\delta^{18}O$ value of -22.2‰ for the research area (Blue diamond shape figure 17; Bowen, 2009). This estimated precipitation isotope ratio based on the model of Bowen (2009) is very similar to the expected ratio based on the Siberian samples.

5.5. Comparing different carbon sources

The different carbon sources (POC, DOC, CH_4 and CO_2) were combined and compared (figure 18). All available carbon data was used in this figure. Correlations between the different carbon sources are given in table 7 and 8 (different water bodies) and table 9 (all water bodies combined). Stream correlations are not given due to the low amount of measurements. Green values in these tables show correlations with a high level of significance (*p*-value < 0.01).

CO_2 and CH_4 concentrations in ponds (figure 18a) show a high positive correlation (0.80; n=83; *p*-value < 0.001). Pond measurements have much higher concentrations for both CO_2 and CH_4 compared to lake and stream data. If lake samples are combined (table 7), no clear correlation was found between CO_2 and CH_4. This is most likely caused by combining different lakes together and the occurrence of active thermokarst at some of the sample locations. Also the small concentrations of greenhouse gases in lakes will decrease the accuracy of the measurements.

If POC is correlated with other carbon sources (figure 18 b, c, and e), there is a clear variance visible between lakes and ponds. The lake data points with increased POC concentrations occur at the samples close to the active thermokarst. These samples do not show an increase in any of the other carbon sources (DOC, CH_4, and CO_2). Pond samples with high POC concentrations also show an increase in DOC, CO_2, and CH_4 concentration.

Correlations of DOC to CH_4 and CO_2 concentrations are shown in figure 18 d and f. None of the lake samples show an exceptional increase in any of these concentrations. The DOC, CH_4, and CO_2 concentrations of pond samples vary much more. The correlation of DOC with CO_2 is highly significant for pond samples (0.58; n=24; *p*-value 0.003). No clear correlation was found between DOC and CH_4 (0.33; n=24; *p*-value 0.117).

Lakes	CO_2	CH_4	POC
DOC [mg C L^{-1}]	0.021	0.27	0.11
POC [mg C L^{-1}]	0.58	0.28	
CH_4 [mg C L^{-1}]	0.047		

Table 7. Correlation coefficient of different carbon sources of all lake samples. Correlations with a green colour have a p-value < 0.01, and are therefore highly significant.

Ponds	CO_2	CH_4	POC
DOC [mg C L^{-1}]	0.58	0.33	0.60
POC [mg C L^{-1}]	0.57	0.56	
CH_4 [mg C L^{-1}]	0.80		

Table 8. Correlation coefficient of different carbon sources of all pond samples. Correlations with a green colour have a p-value < 0.01, and are therefore highly significant.

Lakes, ponds, and streams	CO_2	CH_4	POC
DOC [mg C L^{-1}]	0.82	0.53	0.53
POC [mg C L^{-1}]	0.53	0.53	
CH_4 [mg C L^{-1}]	0.80		

Table 9. Correlation coefficient of different carbon sources of all available samples. Correlations with a green colour have a p-value < 0.01, and are therefore highly significant.

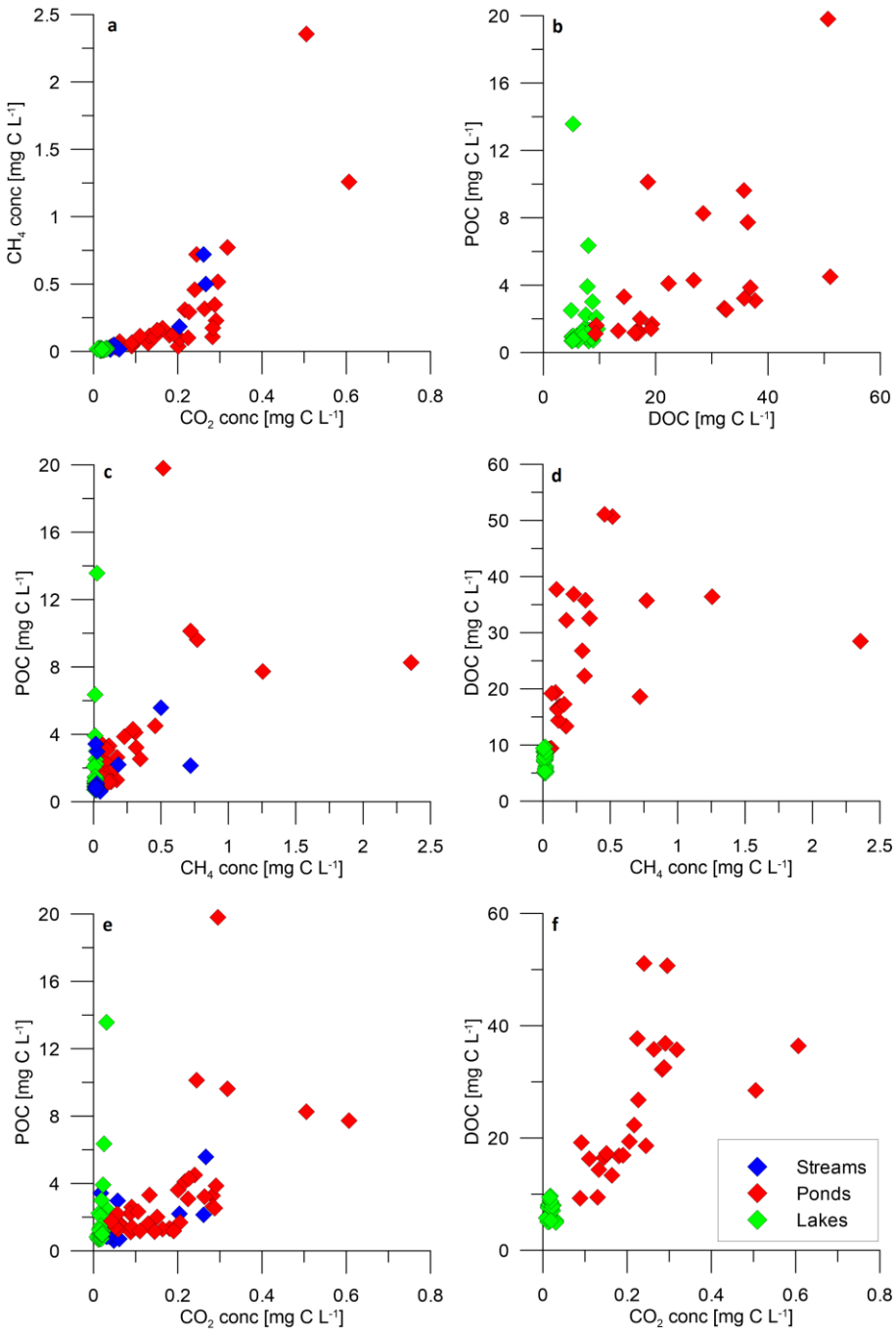

Figure 18. Comparing different carbon concentrations (CO_2, CH_4, POC and DOC). Colours represent the different types of water bodies. All concentrations are in mg C L^{-1}. For some of the carbon concentrations, no stream data was available.

If all measured carbon sources (POC, DOC, CH_4 and CO_2) of the different water bodies are combined (figure 19), a clear variability occurs. All available data is used in this figure. No DOC results were available for the small eastern lake samples (L10-L12), nor for any of the stream sites. The L1 and L3 samples are of special interest due to their position close to active thermokarst. The amounts in percentage for the different water bodies are given in table 10.

The carbon content of the pond sites is significantly higher compared to the other sample locations. The main component of the different forms of carbon present in all water bodies is DOC, followed by POC, CO_2, and CH_4.

Lake carbon sources seem to be consistent for all individual sample locations. Even the L1 and L3 samples do not show a clear increase in total carbon content. The only clear difference between the sites close to the active thermokarst and the other lake sites is the POC content. Percentages of POC for these two sites relative to the total carbon content are higher (25.8% for L1 and 49.6% for L3) than average lake percentages (17.1 and 15.4%), as expected. It is unknown if the active thermokarst is affecting the dissolved gas concentrations at the TK sample.

Besides the differences in total carbon content, a discrepancy was found in the ratio of the different carbon sources between lakes and ponds. CH_4 and CO_2 ratios are higher for pond sites (0.62 (CO_2) and 0.79% (CH_4)) compared to lake sites (0.13 (CO_2) and 0.26% (CH_4)). POC ratios of lakes are higher, although this is mainly caused by the lake sites that are located close to the active thermokarst.

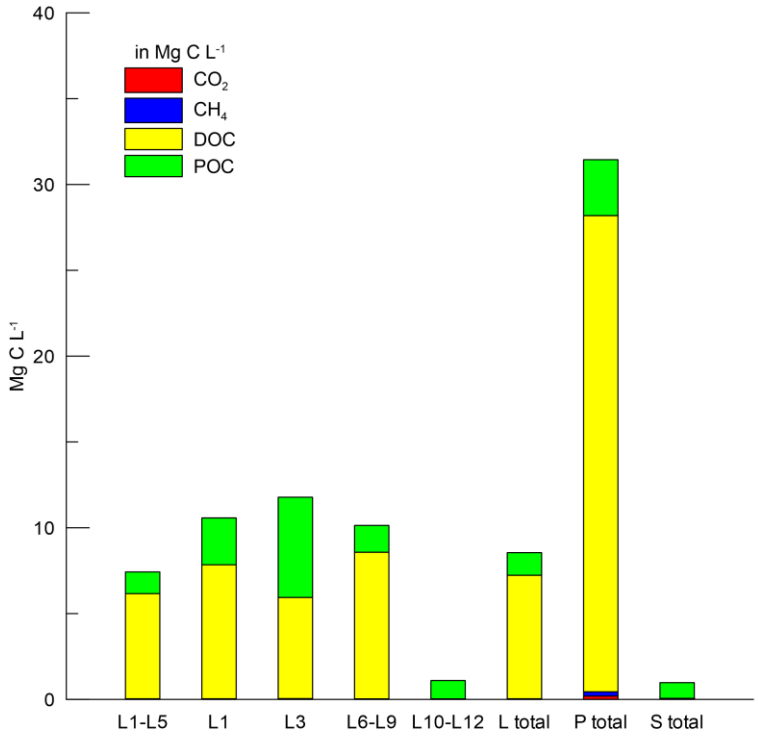

Figure 19. Combined data of DOC, POC, CH_4, and CO_2 concentrations for the different water bodies. Note that there was no DOC data available for the L10-L12 samples and for all the stream samples. Individual pond data is given in figure 20.

Site	Total C conc. [mg C L^{-1}]	CH_4 [%]	CO_2 [%]	POC [%]	DOC [%]
L1-L5	7.43	0.26	0.24	17.1	82.4
L1	10.6	0.17	0.18	25.8	73.8
L3	11.8	0.15	0.23	49.6	50.1
L6-L9	10.1	0.13	0.19	15.4	84.3
P total	31.4	0.79	0.62	10.4	88.2

Table 10. Total carbon concentration and ratios of the different carbon sources of lakes and ponds. Only sites with DOC concentrations are incorporated.

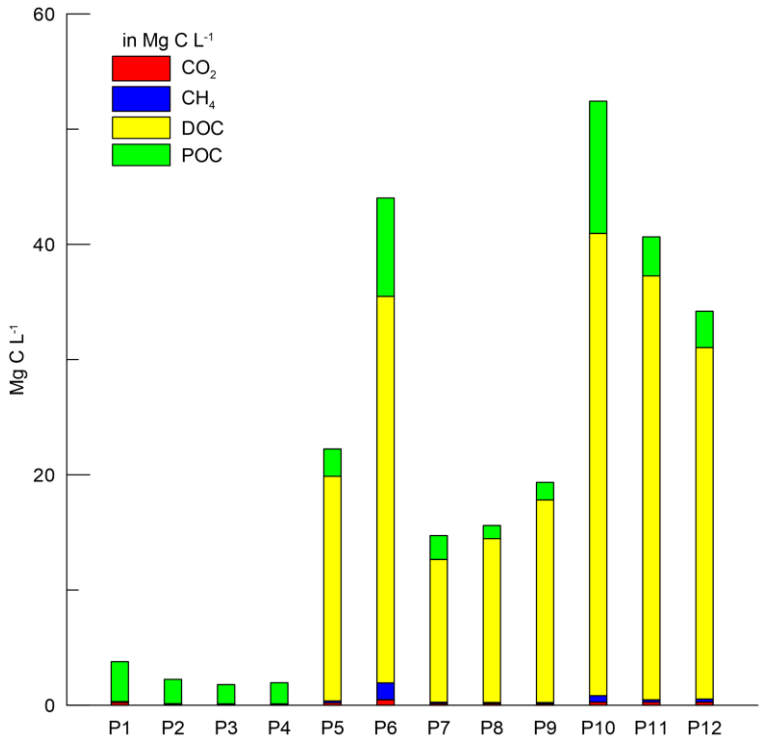

Figure 20. Combined data of carbon sources for the pond sites. Note that no DOC data was available for the first 4 pond locations.

Site	Total C conc. [mg C L^{-1}]	CH_4 [%]	CO_2 [%]	POC [%]	DOC [%]
P5	22.2	0.79	0.90	10.7	87.6
P6	44.0	3.3	1.1	19.4	76.2
P7	14.7	0.79	0.97	14.1	84.2
P8	15.6	0.61	0.91	7.3	91.2
P9	19.3	0.58	0.61	7.9	90.9
P10	52.4	1.1	0.50	21.9	76.5
P11	40.6	0.53	0.64	8.3	90.5
P12	34.2	0.79	0.78	9.2	89.2

Table 11. Concentrations and ratios of the different carbon sources for individual pond sites. Only sites with available DOC concentrations are incorporated.

While the total carbon content of lake samples is consistent for most of the individual sample locations, this is not the case for the different pond sites (figure 20; table 11). No DOC data was available for the samples P1 to P4.

The total carbon concentrations show a lot of variability between different ponds. Highest concentrations are found for site P6 and P10. These sites also show the highest ratio of CH_4 and POC. P6 also shows a high ratio of CO_2, although this is not found for P10. Highest DOC ratios are obtained for pond sites that have a lower total carbon concentration (P8 and P9). The P6 and P10 ponds are the ponds with the smallest surface area, where the P8 and P9 ponds are among the largest and deepest of the measured ponds. Ponds with a smaller surface area tend to have a higher ratio of greenhouse gases, and therefore a higher potential in the release of these gases.

5.5.1. Correlation between carbon source and measured parameters of pond samples

To get a better understanding of the variability in different pond sites, a correlation was created based on the four types of carbon content and the measured field parameters at the sample sites. The results of this correlation can be found in table 12.

	CO2	CH4	POC	DOC
WATER T [°C]	-0.20	-0.25	-0.18	0.12
WIND SPEED 10M [M S^{-1}]	-0.064	-0.25	-0.11	0.16
PH	-0.80	-0.54	-0.53	-0.77
SALINITY [PPT]	0.46	0.28	0.64	0.59
SURFACE AREA [M^2]	-0.56	-0.50	-0.52	-0.48
WATER DEPTH [CM]	-0.27	-0.46	-0.41	-0.38
ACTIVE LAYER [CM]	-0.53	-0.52	-0.42	-0.46
FE [MG L^{-1}]	0.71	0.24	0.53	-0.15
CA [MG L^{-1}]	0.44	0.11	-0.037	-0.79

Table 12. Correlation coefficient between the different carbon contents in ponds and with measured field parameters. Correlations are based on all measurements of this research. Correlations with a green colour have a p-value < 0.01 and are therefore highly significant. Due to a high skewness coefficient of salinity, the correlation with salinity cannot be used to make any assumptions.

A highly significant negative correlation was found for pH will all different carbon sources. Besides pH, also salinity (positive) and surface area (negative) show a highly significant correlation with three of the four carbon sources.

Some important data assumptions are made in order to use Pearson's correlation coefficient. Besides an expected linear relation between the datasets, the datasets are also assumed to be normally distributed. The normality of the datasets can be checked by analysing the Pearson skewness coefficients. This skewness measures the asymmetry of the dataset. If this asymmetry is significantly higher than the standard error of the dataset, the Pearson's correlation coefficient cannot be used to make any assumptions due to the high uncertainty in the dataset.

Although salinity shows a clear positive correlation with the amount of carbon in the pond system, the skewness coefficient (0.61) of salinity is much higher than its standard deviation (0.0039). Due to the small differences in salinity of the pond sites, no conclusions can be taken from the salinity correlations. The skewness index of other measured field parameters and carbon measurements was lower or close to equal to the standard deviation.

The negative correlation with pH is likely caused by the input of carbon into the pond system. The increase in carbon dioxide in a pond system can be a common cause for the decrease of pH (Håkanson, 2006). Aqueous CO_2 reacts with the water and forms H_2CO_3. This carbonic acid can release protons to form (bi)carbonate. The proton is liberated to the water, which decreases the pH. Therefore, the pH of permafrost ponds can be used as an indication for carbon content of the system.

Compared to other Arctic data (Yoshikawa and Hinzman, 2003; Abnizova et al., 2012; Dean et al., 2016), pH values for ponds are very low. These low values can indicate a higher influence of precipitation, as precipitation can decrease the pH of a water body (Dean et al., 2016). Rainfall in arctic regions generally has a pH in the order of 5.5 (Kling et al., 1992b).

Ponds with a smaller surface area have relatively more contact with the surrounding, organic-rich active layer of the permafrost and will therefore have more interaction with the upper soil layer. This can increase the flux of carbon that is flowing from the soil to the ponds. Therefore ponds with a smaller surface area tend to have a higher carbon content, resulting in a negative correlation between surface area and carbon content. The surface area of lakes is less important for the carbon content.

A highly significant negative correlation was obtained between the active layer around the different ponds and the CH_4 and CO_2 concentrations in the water. The active layer around the pond is also highly significantly correlated to the surface area of the ponds (0.75; n=11; *p*-value 0.008; not shown). Bigger ponds have a higher influence in the surrounding soils, resulting in a deeper active layer around these ponds. A deeper active layer may result in a higher potential carbon supply for these ponds, although this does not seem the case in this research area.

6. Conclusion

This research focused on the carbon composition of different freshwater systems in the Northeastern region of Siberia. The carbon data, together with different parameters measured in the field, gave a good understanding in the differences in amount and variability of carbon content that occur between streams, lakes, and ponds.

The gas concentrations of CO_2 and CH_4 were supersaturated in all water bodies while the N_2O values were slightly undersaturated for all water bodies. Due to the small significance of N_2O as a greenhouse gas and the low measured N_2O concentrations, this research mainly focused on CH_4 and CO_2 concentrations. The CO_2 and CH_4 concentrations of pond samples were on average eight times higher compared to lake concentrations. Compared to previous research in the same area, CH_4 concentrations are increased for all water types. Especially a significant increase in CH_4 concentrations of the measured lakes was found. The CO_2 concentrations are similar to previous research and N_2O concentrations are slightly decreased for lakes, streams and ponds.

Flux data was calculated for all three water types, although the pond and stream flux data are likely incorrect due to deficiencies in the approach. The lake flux data of CO_2 seems very similar to other data of Arctic research. The CH_4 fluxes seem to be above average compared to other research results.

POC and DOC concentrations show a clear correlation with the surface area of the water body. Some outliers in POC concentration data were observed in part of the lake samples. The reason for the high POC concentrations in these samples seems to be the occurrence of active thermokarst close to the sample area. Active thermokarst does not seem to have a major effect on the concentrations of the other measured carbon contents, although it is uncertain if DOC, CH_4, and CO_2 conditions at the TK sample location are increased due to active thermokarst.

Each of the lakes show very identical and constant ^{18}O and ^{2}H stable isotope ratios. If these ratios are compared to the pond sites, there is a significant difference. Pond samples show higher, less negative $\delta^{18}O$ and $\delta^{2}H$ values and a far more negative *d* excess. Also the slope of regression of pond samples is less steep (4.29) compared to lake samples (6.28). These differences suggests that ponds are primarily affected by summer precipitation and evapotranspiration whereas lakes are mainly influenced by winter precipitation and thawed ice from ice wedges in the soil.

DOC concentrations are the main carbon content in all different water bodies, followed by POC, CO_2 and CH_4. Ratios of the different carbon types for both streams and lakes seems very similar and constant. For the different pond sites a large variation was found. Ponds show higher ratios of CH_4 and CO_2 compared to lakes and streams, although these ratios are very small (<1%) compared to the POC and DOC ratios.

Permafrost ponds are normally not included in future climatic scenarios. Still, this research shows that permafrost ponds are an important factor in the carbon content of permafrost regions. Not only do they contain a higher carbon content, also the ratio of greenhouse gases (CH_4 and CO_2) in the water is higher compared to lakes and streams. Where most research focusses on the amount of CO_2 release from the permafrost area, this research shows that CH_4 release is equally or even more important as a greenhouse gas due to the high warming potential of methane. The amount of DOC is higher compared to the amount of POC for all of the measured water bodies. Furthermore, a clear correlation was found between the surface area and pH of the freshwater system and the total carbon content of the pond system.

References

Abnizova, A., Siemens, J., Langer, M., & Boike, J. (2012). Small ponds with major impact: The relevance of ponds and lakes in permafrost landscapes to carbon dioxide emissions. *Global Biogeochemical Cycles*, *26*(2).

Abril, G., Bouillon, S., Darchambeau, F., Teodoru, C. R., Marwick, T. R., Tamooh, F., Ochieng Omengo, F., Geeraert, N., Deirmendjian, L., Polsenaere, P., and Borges, A. V. (2015). Technical Note: Large overestimation of pCO 2 calculated from pH and alkalinity in acidic, organic-rich freshwaters. *Biogeosciences*, *12*(1), 67-78.

Alin, S. R., de Fátima FL Rasera, M., Salimon, C. I., Richey, J. E., Holtgrieve, G. W., Krusche, A. V., & Snidvongs, A. (2011). Physical controls on carbon dioxide transfer velocity and flux in low-gradient river systems and implications for regional carbon budgets. *Journal of Geophysical Research: Biogeosciences*, *116*(G1).

Bowen, G. J., Wassenaar, L. I., & Hobson, K. A. (2005). Global application of stable hydrogen and oxygen isotopes to wildlife forensics. *Oecologia*, *143*(3), 337-348.

Bowen, G. J. (2009). The online isotopes in precipitation calculator, version 2.2. *Available from :< http://www. waterisotopes. org*.

Chokurdakh Scientific Tundra Station. (2014, August 26). Retrieved January 17, 2017, from www.eu-interact.org/field-sites/russia-10/chokurdakh/

Ciais, P., C. Sabine, G. Bala, L. Bopp, V. Brovkin, J. Canadell, A. Chhabra, R. DeFries, J. Galloway, M. Heimann, C. Jones, C. Le Quéré, R.B. Myneni, S. Piao and P. Thornton, 2013: Carbon and Other Biogeochemical Cycles. In: *Climate Change 2013: The Physical Science Basis. Contribution of Working Group I to the Fifth Assessment Report of the Intergovernmental Panel on Climate Change* [Stocker, T.F., D. Qin, G.-K. Plattner, M. Tignor, S.K. Allen, J. Boschung, A. Nauels, Y. Xia, V. Bex and P.M. Midgley (eds.)]. Cambridge University Press, Cambridge, United Kingdom and New York, NY, USA.

Climate: Chokurdakh. (2016, October 20). Retrieved from en.climate-data.org/location/30668/

Cole, J. J., & Caraco, N. F. (1998). Atmospheric exchange of carbon dioxide in a low-wind oligotrophic lake measured by. *Limnology and Oceanography*, *43*(4), 647-656.

Collins, S. L., Swinton, S. M., Anderson, C. W., Gragson, T. L., Grimm, N. B., Grove, M., Knapp, A. K. Kofinas, G., Magnuson, J., McDowell, B., Melack, J., Moore, J., Ogden, L., Reichman, O. J., Robertson, G. P., Smith, M. D. & Whitmer, A. (2007). Integrated science for society and environment: A strategic research initiative. *Albuquerque, Long-Term Ecological Research Network, Publication*, (23).

Craig, H. (1961). Isotopic variations in meteoric waters. *Science*, *133*(3465), 1702-1703.

Dean, J. F., Billett, M. F., Baxter, R., Dinsmore, K. J., Lessels, J. S., Street, L. E., Subke, J-A., Tetzlaff, D., Washbourne, I., & Wookey, P. A. (2016). Biogeochemistry of “pristine” freshwater stream and lake systems in the western Canadian Arctic. *Biogeochemistry*, *130*(3), 191-213.

Denfeld, B. A., Frey, K. E., Sobczak, W. V., Mann, P. J., & Holmes, R. M. (2013). Summer CO 2 evasion from streams and rivers in the Kolyma River basin, north-east Siberia. *Polar Research*, *32*.

Driscoll, C. T., & Schecher, W. D. (1990). The chemistry of aluminum in the environment. *Environmental Geochemistry and Health*, *12*(1-2), 28-49.

EPA, Environmental Protection Agency, United States, Understanding Global Warming Potentials. (2017, February 14). Retrieved March 6, 2017, from https://www.epa.gov/ghgemissions/understanding-global-warming-potentials.

Fenton, N., & Neil, M. (2012). *Risk assessment and decision analysis with Bayesian networks*. Crc Press.

Fondriest Environmental, Inc. "pH of Water." Fundamentals of Environmental Measurements. 19 Nov. 2013. Web. < http://www.fondriest.com/environmental-measurements/parameters/water-quality/ph/ >.

Friedlingstein, P., Cox, P., Betts, R., Bopp, L., Von Bloh, W., Brovkin, V., Cadule, P., Doney, S., Eby, M., Fung, I., Bala, G., John, J., Jones, C., Joos, F., Kato, T., Kawamiya, M., Knorr, W., Lindsay, K., Matthews, H.D., Raddatz, T., Rayner, P., Reick, C., Roeckner, E., Schnitzler, K.-G., Schnur, R., Strassmann, K., Weaver, A.J., Yoshikawa, C. and Zeng, N. (2006). Climate-carbon cycle feedback analysis: Results from the C4MIP model intercomparison. *Journal of Climate*, *19*(14), 3337-3353.

Gibson, J. J., Edwards, T. W. D., Bursey, G. G., & Prowse, T. D. (1993). Estimating evaporation using stable isotopes: quantitative results and sensitivity analysis for two catchments in northern Canada. *Hydrology Research*, *24*(2-3), 79-94.

Gibson, J. J., & Edwards, T. W. D. (2002). Regional water balance trends and evaporation-transpiration partitioning from a stable isotope survey of lakes in northern Canada. *Global Biogeochemical Cycles*, *16*(2).

Gonçalves-Araujo, R., Granskog, M. A., Bracher, A., Azetsu-Scott, K., Dodd, P. A., & Stedmon, C. A. (2016). Using fluorescent dissolved organic matter to trace and distinguish the origin of Arctic surface waters. *Scientific Reports*, *6*.

Goovaerts, A. (2016). *An explorative study of carbon sources and greenhouse gas emissions in thermokarst lakes and rivers using stable isotopes (Chokurdakh, Yakutsk, Russia)* (Unpublished Master's thesis, Katholieke Universiteit Leuven, Belgium).

Goulsbra, C. S., Evans, M. G., & Allott, T. E. (2016). Rates of CO2 efflux and changes in DOC concentration resulting from the addition of POC to the fluvial system in peatlands. *Aquatic Sciences*, *78*(3), 477-489.

Guo, L., Ping, C. L., & Macdonald, R. W. (2007). Mobilization pathways of organic carbon from permafrost to arctic rivers in a changing climate. Geophysical Research Letters, 34(13).

Håkanson, L. (2006). The relationship between salinity, suspended particulate matter and water clarity in aquatic systems. *Ecological Research*, *21*(1), 75-90.

Holgerson, M. A., & Raymond, P. A. (2016). Large contribution to inland water CO2 and CH4 emissions from very small ponds. *Nature Geoscience*.

IPCC, 2013: Climate Change 2013: The Physical Science Basis. Contribution of Working Group I to the Fifth Assessment Report of the Intergovernmental Panel on Climate Change [Stocker, T.F., D. Qin, G.-K. Plattner, M. Tignor, S.K. Allen, J. Boschung, A. Nauels, Y. Xia, V. Bex and P.M. Midgley (eds.)]. Cambridge University Press, Cambridge, United Kingdom and New York, NY, USA, 1535 pp

Johnson, H. K., Højstrup, J., Vested, H. J., & Larsen, S. E. (1998). On the dependence of sea surface roughness on wind waves. *Journal of Physical Oceanography*, *28*(9), 1702-1716.

Jonsson, C. E., Leng, M. J., Rosqvist, G. C., Seibert, J., & Arrowsmith, C. (2009). Stable oxygen and hydrogen isotopes in sub-Arctic lake waters from northern Sweden. *Journal of Hydrology*, *376*(1), 143-151.

Kendall, C., & McDonnell, J. J. (Eds.). (2012). *Isotope tracers in catchment hydrology* (pp. 51-86). Amsterdam, Elsevier.

Kling, G. W., Kipphut, G. W., & Miller, M. C. (1992a). The flux of CO2 and CH4 from lakes and rivers in arctic Alaska. In *Toolik Lake* (pp. 23-36). Springer Netherlands.

Kling, G. W., O'Brien, W. J., Miller, M. C., & Hershey, A. E. (1992b). The biogeochemistry and zoogeography of lakes and rivers in arctic Alaska. In *Toolik Lake* (pp. 1-14). Springer Netherlands.

Laurion, I., Vincent, W. F., MacIntyre, S., Retamal, L., Dupont, C., Francus, P., & Pienitz, R. (2010). Variability in greenhouse gas emissions from permafrost thaw ponds. *Limnology and Oceanography*, *55*(1), 115-133.

Lenhard, W. & Lenhard, A. (2014). *Hypothesis Tests for Comparing Correlations*. available: https://www.psychometrica.de/correlation.html. Bibergau (Germany): Psychometrica. DOI: 10.13140/RG.2.1.2954.1367

Lim, D. S., & Douglas, M. S. (2003). Limnological characteristics of 22 lakes and ponds in the Haughton Crater region of Devon Island, Nunavut, Canadian High Arctic. Arctic, Antarctic, and Alpine Research, 35(4), 509-519.

Mackenzie, F. T. (1980). Global Carbon Cycle. *Carbon Dioxide Effects Research and Assessment Program*, 360.

Neff, J. C., Finlay, J. C., Zimov, S. A., Davydov, S. P., Carrasco, J. J., Schuur, E. A. G., & Davydova, A. I. (2006). Seasonal changes in the age and structure of dissolved organic carbon in Siberian rivers and streams. *Geophysical Research Letters*, *33*(23).

Parmentier, F. J. W., Van Der Molen, M. K., Van Huissteden, J., Karsanaev, S. A., Kononov, A. V., Suzdalov, D. A., Maximov, T. C. & Dolman, A. J. (2011). Longer growing seasons do not increase net carbon uptake in the northeastern Siberian tundra. *Journal of Geophysical Research: Biogeosciences*, *116*(G4).

Ran, L., Lu, X. X., Yang, H., Li, L., Yu, R., Sun, H., & Han, J. (2015). CO2 outgassing from the Yellow River network and its implications for riverine carbon cycle. *Journal of Geophysical Research: Biogeosciences*, *120*(7), 1334-1347.

Schaefer, K., Zhang, T., Bruhwiler, L., & Barrett, A. P. (2011). Amount and timing of permafrost carbon release in response to climate warming. *Tellus B*,*63*(2).

Schirrmeister, L., Pestryakova, L., Wetterich, S., & Tumskoy, V. (2012). Joint Russian-German polygon project: East Siberia 2011-2014; the expedition Kytalyk 2011. *Berichte zur Polar-und Meeresforschung= Reports on polar and marine research*, *653*

Schuur, E. A., Bockheim, J., Canadell, J. G., Euskirchen, E., Field, C. B., Goryachkin, S. V., Hagemann, S., Kuhry, P., Lafleur, P.M., Lee, H., Mazhitova, G., Nelson, F.E., Rinke, A., Romanovsky, V.E., Shiklomanov, N., Tarnocai, C., Venevsky, S., Vogel, J.G. and Zimov, S.A. (2008). Vulnerability of permafrost carbon to climate change: implications for the global carbon cycle. *BioScience*, *58*(8), 701-714.

Schuur, E. A., & Abbott, B. (2011). Climate change: High risk of permafrost thaw. *Nature*, *480*(7375), 32-33.

Shacklette, H. T., & Boerngen, J. G. (1984). Element concentrations in soils and other surficial materials of the conterminous United States.

Standard Methods for the Examination of Water and Wastewater, 20th edition, 1999. Retrieved January 17, 2017, from http://www.chemiasoft.com/chemd/salinity_calculator

Tarnocai, C., Canadell, J. G., Schuur, E. A. G., Kuhry, P., Mazhitova, G., & Zimov, S. (2009). Soil organic carbon pools in the northern circumpolar permafrost region. *Global biogeochemical cycles*, *23*(2).

Teodoru, C. R., Del Giorgio, P. A., Prairie, Y. T., & Camire, M. (2009). Patterns in pCO2 in boreal streams and rivers of northern Quebec, Canada. *Global Biogeochemical Cycles*, *23*(2).

Thornton, B. F., Wik, M., & Crill, P. M. (2016). Double-counting challenges the accuracy of high-latitude methane inventories. *Geophysical Research Letters*.

Van Huissteden, J., Maximov, T. C., & Dolman, A. J. (2005). High methane flux from an arctic floodplain (Indigirka lowlands, eastern Siberia). *Journal of Geophysical Research: Biogeosciences*, *110*(G2).

Vonk, J. E., Tank, S. E., Bowden, W. B., Laurion, I., Vincent, W. F., Alekseychik, P., Amyot, M., Billet, M. F., Canário, J., Cory, R. M., Deshpande, B. N., Helbig, M., Jammet, M., Karlsson, J., Larouche, J., MacMillan, G., Rautio, M., Walter Anthony, K. M., & Wickland, K.P. (2015). Reviews and syntheses: Effects of permafrost thaw on Arctic aquatic ecosystems. *Biogeosciences*, *12*(23), 7129-7167.

Wik, M., Varner, R. K., Anthony, K. W., MacIntyre, S., & Bastviken, D. (2016). Climate-sensitive northern lakes and ponds are critical components of methane release. *Nature Geoscience*.

Yamamoto, S., Alcauskas, J. B., & Crozier, T. E. (1976). Solubility of methane in distilled water and seawater. *Journal of Chemical and Engineering Data*, *21*(1), 78-80.

Yoshikawa, K., & Hinzman, L. D. (2003). Shrinking thermokarst ponds and groundwater dynamics in discontinuous permafrost near Council, Alaska. *Permafrost and Periglacial Processes*, *14*(2), 151-160.

Zhang, T., Barry, R. G., Knowles, K., Heginbottom, J. A., and Brown, J. (1999). Statistics and characteristics of permafrost and ground-ice distribution in the Northern Hemisphere 1. *Polar Geography*, *23*(2), 132-154.

Acknowledgement

First and foremost, I would like to thank Josh Dean for giving me the opportunity to join the field work in Kytalyk and all his help during this guided research. I would like to thank Jack Middelburg and Jorien Vonk for their supervision. Special thanks to Ove Meisel, Richard van Logtestijn and Josh for creating unforgettable memories during the field work. Thanks for helping me survive in the mosquito nightmare. I also thank Steven Bouillon, Thibault Lambert, Alberto Viera Borges, and Marc-Vincent Commarieu for their help during the lab work, and giving me the opportunity to work in their lab at the Université de Liège. Finally I thank Richard for helping me during the process of the POC measurements.

Appendix 1 – Coordinates and notes of the sample locations in the Kytalyk area

Site	°N	°E	Note
P1	70.83082	147.4749	
P2	70.83150	147.4746	
P3	70.83304	147.4742	
P4	70.83335	147.4742	
P5	70.83398	147.4745	
P6	70.83459	147.4744	very small pond with a very dark, black colour
P7	70.83479	147.4742	
P8	70.83483	147.4742	
P9	70.83675	147.4725	
P10	70.83703	147.4734	
P11	70.83862	147.4727	
P12	70.83871	147.4740	
L1	70.82892	147.4420	Closely located to the active thermokarst (TK) sample site
L2	70.83285	147.4281	
L3	70.83022	147.4138	Active thermokarst visible near L3
L4	70.82754	147.4219	
L5	70.82684	147.4316	
L6	70.84735	147.4090	
L7	70.84583	147.3998	
L8	70.84852	147.3993	
L9	70.84927	147.4069	
L10	70.84869	147.4177	
L11	70.84818	147.4260	
L12	70.84756	147.4223	
S1	70.83167	147.5173	Pond site that is closely located to the stream, probably connected to the stream during high water
S2	70.83138	147.5176	
S3	70.82997	147.5118	samples of the stream were taken with an inflatable boat to get samples from the middle of the river
S4	70.82890	147.5048	samples were taken in the outer corner of the river
Kytalyk	70.82784	147.4904	Base camp

Appendix 2 – Measured field parameters of the different ponds and lakes

Site	Size [m]	Area [m^2]	Depth [cm]	Measured active layer [cm]
P1	8 by 12	96	40	X
P2	6 by 6	36	20	37.5
P3	13 by 12	156	20	48
P4	11 by 15	165	20	51
P5	8 by 12	96	22	39
P6	0.6 by 5	3	12	36
P7	8 by 7	56	20	48
P8	24 by 6	144	30	52
P9	8 by 30	240	40	50
P10	4 by 8	32	15	43
P11	6 by 10	60	30	45
P12	13 by 9	117	20	46
S1	15 by 4	60	30	X
Big lake (L1, L2, L3, L4, & L5)		511189		
Smaller western lake (L6, L7, L8, & L9)		140596		
Smaller eastern lake (L10, L11, & L12)		41718		

Appendix 3 – Field parameters and timing of the sample measurements

Site	Date [d/m/y]	Time	EC [µS/cm]	Temp [degrees]	pH	Temp [degrees]	Stable isotope sample
P12	31-7-2016	16:00	23.4	13.1	5.28	13.4	
P11	31-7-2016	17:00	23.1	14.1	5.35	14.4	X
P10	31-7-2016	17:00	52.3	14.6	5.38	14.7	
P9	31-7-2016	17:00	24.2	13.5	6.33	13.6	
P8	31-7-2016	18:00	24.1	13.6	6.59	14	X
P7	31-7-2016	18:00	15.1	14	6.2	14.4	
P6	31-7-2016	18:00	28.2	12.7	5.14	13.2	
P5	31-7-2016	18:00	19.8	15.3	5.94	14.8	
P4	31-7-2016	19:00	14.8	15	6.67	15.1	
P3	31-7-2016	20:00	15.3	13.1	6.31	13.4	X
P2	31-7-2016	21:00	14.7	13.7	5.94	13.8	X
P1	31-7-2016	21:00	38.8	13.9	5.68	14.3	X
S1	1-8-2016	11:00	48.6	14.2	6.17	14.5	X
S2	1-8-2016	11:00	48.2	14.8	6.93	15	
S3	1-8-2016	12:00	76.6	15.4	7.36		X
S4	1-8-2016	13:00	47.6	14.2	7.16		
L1	1-8-2016	15:00	205	14.8	7.62		X
L2	1-8-2016	15:00	200	15.9	8.14		
L3	1-8-2016	16:00	209	17.2	7.96		X
L4	1-8-2016	16:00	200	15.3	7.85		X
L5	1-8-2016	17:00	201	14.7	8.06		
L6	2-8-2016	12:00	33.7	12.1	7.3	12.3	X
L7	2-8-2016	12:00	28	11.8	7.44	12.2	
L8	2-8-2016	12:00	28.2	12.1	7.33	12.4	X
L9	2-8-2016	13:00	27.7	12.8	7.26	13	
L12	2-8-2016	14:00	16	13	6.81	13.2	X
L10	2-8-2016	15:00	15.7	12.9	6.64	13.1	X
L11	2-8-2016	15:00	16	13	6.85	13.3	
P12	3-8-2016	10:25	24.1	13.9	5.38	13.4	
P11	3-8-2016	10:45	25.3	15.2	5.26	15.3	X
P10	3-8-2016	11:00	48.1	17.3	5.35	17.6	
P9	3-8-2016	11:20	23.4	14.4	5.87	14.2	
P8	3-8-2016	11:45	25.5	14.9	6.04	15.2	X
P7	3-8-2016	12:10	16.2	17.8	5.74	17.7	
P6	3-8-2016	12:30	26.8	17.3	5.06	17.4	
P5	3-8-2016	14:24	24.4	20.8	5.45	21.1	
P4	3-8-2016	14:39	15.1	21.5	5.98	21.8	
P3	3-8-2016	14:59	15.5	21.6	6.13	22.2	X
P2	3-8-2016	15:08	14.8	22.3	5.91	22.5	X
P1	3-8-2016	15:19	36.9	21.7	5.58	21.8	X

L1	5-8-2016	10:53	203	14.3	7.71	14.5	X
L2	5-8-2016	11:14	202	14.6	8.06	14.9	
L3	5-8-2016	11:33	204	14	7.78	14.3	X
L4	5-8-2016	11:58	202	14.2	8.18	14.5	
L5	5-8-2016	12:13	202	14.1	8.13	14.4	
S2	5-8-2016	15:00	47	14.6	7.84	14.9	
S1	5-8-2016	15:15	48.7	14.5	7.05	14.8	X
S4	5-8-2016	18:19	46.2	14.6	7.51	14.9	
S3	5-8-2016	18:45	52.7	13.5	7.6	13.8	X
P1	6-8-2016	14:02	40.8	10.7	5.84	10.9	X
P2	6-8-2016	14:12	15.5	11.1	6.13	11.4	X
P3	6-8-2016	14:18	17.7	11.1	6.2	11.4	X
P4	6-8-2016	14:25	17.3	11.1	6.14	11.4	
P5	6-8-2016	14:36	25.5	10.2	5.74	10.5	
P6	6-8-2016	14:47	25.2	8.9	5.32	9.2	
P7	6-8-2016	14:58	16.2	10.4	5.85	10.8	
P8	6-8-2016	15:09	32.9	10.6	5.92	10.9	X
P9	6-8-2016	15:19	32.1	10.8	5.98	11.1	
P10	6-8-2016	15:25	42	9.9	5.57	10.2	
P11	6-8-2016	15:38	25.2	10.1	55.4	10.4	X
P12	6-8-2016	15:44	22.8	10.3	5.36	10.6	
L11	7-8-2016	11:14	17.3	13.1	6.92	13.3	
L12	7-8-2016	11:28	17	13.2	6.99	13.5	
L6	7-8-2016	11:41	28.8	13	6.87	13.3	
L7	7-8-2016	11:58	28.8	12.8	6.95	13.1	
L8	7-8-2016	12:20	28.8	13.3	7.04	13.6	X
L9	7-8-2016	12:40	28.6	13.6	6.92	14	
L10	7-8-2016	12:58	17.1	14.2	6.94	14.5	X
S1	8-8-2016	10:34	45.8	13.3	6.68	13.7	X
S2	8-8-2016	10:46	49.6	14.7	6.98	14.9	
S3	8-8-2016	11:19	49.8	14.2	7.17	14.6	X
S4	8-8-2016	13:00	53.8	15.2	7.2	15.6	
L1	8-8-2016	14:45	205	14.3	7.85	14.6	X
L2	8-8-2016	15:02	204	15.6	8.15	16	X
L3	8-8-2016	15:26	206	17.2	7.88	17.6	
L4	8-8-2016	15:48	203	15.4	8.19	15.8	X
L5	8-8-2016	16:00	203	14.6	8.35	14.7	
L11	9-8-2016	11:30	17.4	13.7	6.03	13.9	X
L12	9-8-2016	11:44	17.3	13.6	6.25	13.9	X

L10	9-8-2016	11:59	17.1	13.6	6.26	13.9	X
L9	9-8-2016	12:25	29.5	13.6	6.64	13.9	X
L8	9-8-2016	12:38	29.5	13.5	6.61	13.8	X
L7	9-8-2016	12:56	29.2	13.5	6.69	13.7	
L6	9-8-2016	13:15	29.3	13.6	6.88	13.8	
TK	8-8-2016						X
min			14.7	8.9	5.06	9.2	
max			209	22.3	55.4	22.5	